Use of sub-grid approaches in the modelling of estuaries with salt marsh systems

Produced within Defra Project FD1905 (EstProc)

J R Spearman
J Baugh
M J McCoy

Report TR 138
Rev 1.0
January 2004

HR Wallingford

Document Information

Project	Estuary Processes Research Project (EstProc), Defra Project 1905
Report title	Use of sub-grid approaches in the modelling of estuaries with salt marsh systems
Client	Defra/Environment Agency Flood and Coastal Defence R&D Programme
Client Representative	Dr Jonathan Rogers, Mouchel
Project No.	CBS0022
Report No.	TR138
Doc. ref.	TR138-Use of sub-grid rev 1-0.doc
Project Manager	Dr J Spearman
Project Sponsor	R L Soulsby

Document History

Date	Revision	Prepared	Approved	Authorised	Notes
30/01/04	0.0	J Spearman	J Baugh	R J S Whitehouse	
16/02/04	1.0	J Spearman	J Baugh	R J S Whitehouse	

Prepared .....

Approved .....

Authorised .....

 January 2004

Summary

Use of sub-grid approaches in the modelling of estuaries with salt marsh systems

J R Spearman
J Baugh
M J McCoy

Report TR138
January 2004

Introduction

Dendritic systems (which for the sake of this study effectively means saltmarsh and mudflats, although the general principles apply to all such systems) have irregular bathymetry which can vary significantly over length-scales of 1m or less. These small length scales are considerably less than the practically viable scales of 2D flow model grids for applied modelling. For (non-research) estuary modelling scales are typically of the order of 50-100m in estuaries (and greater for large systems).

The normal course of action open to the numerical modeller is to enhance the grid resolution over the (dendritic) mudflat/saltmarsh up to the point where the flow within the system becomes acceptably similar to the observations. However higher grid resolutions lead to larger numbers of grid cells which can lead to impracticably long run times.

The subject of this report, produced within Defra Project FD1905 (EstProc), is the development of an approach to include the effect of the small-scale bathymetric variation on flows without increasing the grid resolution. This type of approach is termed "sub-grid" modelling. The motivation behind the research is to develop a means of including the effect of the dendritic/sub-grid bathymetric variation on the current flows whilst keeping run times to satisfactory levels.

Methodology

The method used in this study to include the effect of the small-scale bathymetric variation on flows is based on work by Defina (2000) and makes use of a facility in the TELEMAC-2D software which allows the porosity of flow through a model grid cell to be defined and altered on every time step. On the basis of high resolution LiDAR data a sub-grid bathymetry was derived at every grid cell and this sub-grid bathymetry was used to calculate the grid cell porosity. The TELEMAC-2D model then made use of the calculated porosity values in the hydrodynamic calculation. In this way the effect of the sub-grid bathymetry on the flow was represented.

The test case used was that of Salcott Creek, a tributary of the Blackwater, near Abbotshall. This Creek is a tributary of the Blackwater Estuary and is characterised by extensive areas of saltmarsh.

A model grid with very fine resolution over the saltmarsh area (of resolution 3-6m) was used to generate model results which were assumed to be "as close as possible" to the observations and to represent a "best" approximation of the estuary system. By reducing the grid resolution (to 20m and 40m) over the saltmarsh areas of the estuary the accuracy of the model was reduced.

Summary continued

The objective of the study was to implement the sub-grid technique to see whether this technique reduced the errors in the model prediction associated with the coarser resolution. The performance of the various approaches taken was determined through quantification of model skill using the Brier Skill Score.

Conclusions

The studies described suggest that the sub-grid methodology will improve the representation of flows both within saltmarsh systems and in estuaries containing such systems. For a given resolution, however, the results of this study suggest that the method can only *partially* overcome the inaccuracy introduced by coarser resolution. The best results using the method showed significant improvement for (20m) grid cells 20 times larger (in area) than the fine grid cell. However, for (40m) grid cells around 80 times larger (in area) than the fine grid cell the best results using the method still improved the model results but the poorer connectivity resulting from this coarser grid reduced the effectiveness of the method.

The method was consistently successful at improving flows within the saltmarsh but was less successful at improving subtidal flows. Moreover, outside of the saltmarsh the improvements in accuracy due to the method varied from significant improvement to significant deterioration in accuracy and no clear pattern could be observed with variation in location.

An algorithm has been devised showing how the sub-grid methodology can be implemented in computational flow models.

Contents

Contents continued

Figures

Appendices

1. Introduction to dendritic systems

Dendritic systems (which for the sake of this study effectively means saltmarsh and mudflats, although the general principles apply to all such systems) have irregular bathymetry which can vary significantly over length-scales of 1m or less. These small length scales are considerably less than the practically viable scales of 2D flow model grids for applied modelling. For (non-research) estuary modelling scales are typically of the order of 50-100m in estuaries (and greater for large systems)

The inability of applied models to reproduce the small-scale variation in bed levels can result in a poor overall description of flow through grid cells representing flow through highly varied since the bed is represented by a single level throughout the cell. A single level cannot both adequately represent the total storage and the deepest channel through the cell. Usually the bed level is some averaged value (see Figure 1) meaning that the model represents flow through the grid cell later in the tide than the real situation. This can result in a poor representation of flow through the (saltmarsh or mudflat) system as a whole especially as it drys and wets. Moreover in an estuary system or tidal inlet dominated by significant and small-scale bathymetric variation these problems can result in a generally poor reproduction of flows in the system.

The normal course of action open to the numerical modeller is to enhance the grid resolution over the (dendritic) mudflat/saltmarsh up to the point where the flow within the system becomes acceptably similar to the observations. However higher grid resolutions lead to larger numbers of grid cells which can lead to impracticably long run times.

The subject of this report, produced within Defra Project FD1905 (EstProc) is the development of an approach to include the effect of the small-scale bathymetric variation on flows without increasing the grid resolution. This type of approach is termed “sub-grid” modelling. The motivation behind the research is to develop a means of including the effect of the dendritic/sub-grid bathymetric variation on the current flows whilst keeping run times to satisfactory levels.

2. A review of sub-grid approaches

2.1 INTRODUCTION

Various authors have applied sub-grid approaches and in this Chapter we review two approaches which are particularly relevant to this study: those of Miles *et al* (1989) and Defina (2000).

2.2 MILES *ET AL* (1989)

The approach of Miles was to explicitly represent the sub-grid bathymetry in the model. A finite difference model, in this case the HR Wallingford model TIDEWAY, was modified so that the flow in the U direction (i.e. parallel to the model grid "rows") and V direction (ir parallel to the model grid "columns") was calculated using a sub-grid bathymetry instead of a single averaged value. The bathymetric data was analysed beforehand to provide a look up table (which the model consequently referred to during run time). The look up table allowed a rapid calculation of cell grid U and V flow cross section areas for a given water level.

The sub-grid model was applied to the case of the Mersey Estuary, an estuary marked in its upper reaches by meandering channels that normally require fine resolution to accurately model the tidal propagation. The application of the sub-grid method showed that tidal propagation and intertidal exposure were much improved for a given grid resolution when the method was used, although the method resulted in run times that were significantly increased.

The sub-grid approach of Miles *et al* was compared to a standard model during a modelling exercise of Tollesbury Creek using the HR Tideway model (Chesher *et al*, 1995). Tollesbury Creek, a small tributary of the Blackwater Estuary, was the location for a proposed managed realignment scheme (which has now been implemented). The creek system is dominated by large expanses of salt marsh. The sub-grid bathymetry in this case was assumed to be homogeneous for the whole saltmarsh and was defined using aerial photography. The modelling exercise attempted to calibrate the sub-grid and standard models against observations of water levels and tidal currents within the creek. The sub-grid model performed significantly better at this exercise than the standard model.

2.3 DEFINA (2000)

Defina's idea was to include the effect of subgrid variation in the flow model equations. Defina considered the effect of dry areas on the flow through a grid cell and produced the following equations for continuity and momentum:

continuity

$$\eta \frac{\partial h}{\partial t} + \frac{\partial q_x}{\partial x} + \frac{\partial q_y}{\partial y} = S \tag{1}$$

momentum

$$\rho \frac{\partial q_x}{\partial t} + \rho \frac{\partial}{\partial x}\left(\varepsilon_{xx} \frac{q_x q_x}{Y} \right) + \rho \frac{\partial}{\partial y}\left(\varepsilon_{xy} \frac{q_x q_y}{Y} \right) - \rho \left(\frac{\partial R_{xx}}{\partial x} + \frac{\partial R_{xy}}{\partial x} \right) \tag{2}$$

$$-\tau_{sx}+\tau_{bx}+\rho gY\frac{\partial h}{\partial x}-\rho\frac{S}{\eta}U_x\big|_{z=h}=0$$

$$\rho\frac{\partial q_y}{\partial t}+\rho\frac{\partial}{\partial x}\left(\varepsilon_{xy}\frac{q_x q_y}{Y}\right)+\rho\frac{\partial}{\partial y}\left(\varepsilon_{yy}\frac{q_y q_y}{Y}\right)-\rho\left(\frac{\partial R_{xy}}{\partial x}+\frac{\partial R_{xy}}{\partial x}\right) \tag{3}$$

$$-\tau_{sy}+\tau_{by}+\rho gY\frac{\partial h}{\partial y}-\rho\frac{S}{\eta}U_y\big|_{z=h}=0$$

where q_x and q_y is the depth-integrated flow in the x and y directions,
S is a source/sink term (=0 for the purposes of this study)
ρ is the density of seawater
h is the free surface elevation
R_{xx} , R_{xy} and R_{yy} are given by,

$$R_{xx}=2\nu_e\frac{\partial q_x}{\partial x}\qquad R_{yy}=2\nu_e\frac{\partial q_y}{\partial y}\qquad \text{an}\qquad R_{xy}=\nu_e\left(\frac{\partial q_x}{\partial y}+\frac{\partial q_y}{\partial x}\right)$$

U_x and U_y are the x and y components of the flow velocity
Y is the "effective" depth i.e. the water volume per unit area
η is the wet fraction of the model grid cell – which will refer to as the "porosity"

ε_{xx} , ε_{xy} , ε_{yy} are momentum correction factors which as a first approximation can be taken as approximately equal to 1 (Definas, 2000)

These equations are similar to the normal shallow water counterparts except that Y and η replace the parameters D (water depth) and 1, respectively. As the sub-grid variation becomes small Y tends to D and η tends to 1.

Defina approached the characterisation of the sub-grid variation by assuming that the sub-grid variation was normally distributed. This assumption leads to the following values of Y and η:

$$\eta=\frac{1}{2}\left\{1+erf\left[2\left(h-h_b\right)/a_r\right]\right\} \tag{4}$$

$$Y=a_r\left\{\eta\left(\frac{h-h_b}{a_r}\right)+\frac{1}{4\sqrt{\pi}}\exp\left[-4\left(\frac{h-h_b}{a_r}\right)^2\right]\right\} \tag{5}$$

where *erf* is the error function,
h_b is the local bed elevation
a_r is the length-scale of the sub-grid bathymetric variation in bed level (≈ 2σ where σ is the standard deviation of the sub-grid bathymetric variation)

3. Methodology

3.1 INTRODUCTION

The method proposed is essentially the adaptation of the Miles method to a finite element model by using Defina's ideas about porosity in the flow model equations. The methodology makes use of the TELEMAC-2D software (see Appendix 1) which has an option to implement a user-defined distribution of porosity across the model grid. The software implements the continuity equation (Equation 4) of Defina with the added merit that the TELEMAC version implements this equation by putting porosity within the $\partial/\partial t$, $\partial/\partial x$, and $\partial/\partial y$ terms thus improving the mass conservation of the technique. TELEMAC-2D solves the momentum equation in a non-conservative manner and it can be shown that the treatment is equivalent with the addition of porosity (Hervouet *et al*, 2000).

The porosity option allows use of the methodology of Defina to represent sub-grid variation. The difference here is that instead of assuming a gaussian distribution for the sub-grid variation as Defina does, we use a method whereby LiDAR data (which stands for 'Light Detection and Ranging', a type of remote sensing), which resolves the sub-grid variation down to scales of around 2m, is used directly to characterise the variation of the bed.

Section 3.2 below discusses the approach used to characterise the sub-grid variation while Section 3.3 describes the method used to calculate the "porosity" corresponding to a particular sub-grid distribution.

3.2 USE OF LIDAR TO CHARACTERISE SUB-GRID VARIATION

Let the number of data points within a search radius R of the TELEMAC node $\underline{x}$ be N. Assume that the distribution of bed levels (z_i , I=1, 2, …,N) within this area, is homogeneous. Then the probability of having the bed level z_i at $\underline{x}$ is $\boldsymbol{f}(z)=1/N$. We can use this probability density function $\boldsymbol{f}$ to estimate the "expected" distribution of bed level for a cross-section at $\underline{x}$. This gives an expected cross-section composed of all bed levels z_i such that each level z_i characterizes $1/N^{th}$ of the cross-section (Figure 2).

3.3 CALCULATION OF POROSITY

Porosity is given by area of "expected" cross-section divided by the whole area down to the minimum bottom level. Consider the example in Figure 3. Let A be the area of the expected cross-section between the water level and the bed and let Area B be the area of the whole rectangle. The porosity is then given by A/B.

The best results were obtained when porosity was constrained by a lower limit and tests indicated that the most suitable lower limit was in the region of 0.5. This value is equivalent to assuming that the channels within the saltmarsh are concave, i.e. "V" or "U"shaped.. The results presented and discussed below mostly utilise a lower porosity limit of 0.5 but a sensitivity test (Simulation 6) is included which use a lower limit for porosity of 0.1.

3.4 SELECTION OF THE BATHMETRY SEARCH RADIUS

The consideration of the search radius over which the bathymetry local to any given model grid cell is considered is an important part of the method. It is clear that the

larger the search radius, the larger the range of variation in the bathymetry and the lower the locally deepest bed level will be. The range of local bed variation represented at a model cell, should ideally match the range of bathymetric variation for the area represented by the model cell. Two approaches are used to define how this search radius is chosen: empirically by comparing the model results using different search radii (see Tables 2 and 3) and semi-analytically by considering the areas corresponding to the model elements and the different search radii (Section 5.4).

4. Test case

4.1 INTRODUCTION

The test case used was that of Salcott Creek, a tributary of the Blackwater, near Abbotshall (Figures 4). This Creek is a tributary of the Blackwater Estuary and is characterised by extensive areas of saltmarsh. Salcott Creek was the location for a study of managed realignment sponsored by the Environment Agency (HR Wallingford, 2001) which has led to a successful realignment scheme.

The study included the following:

- the collection of LiDAR data area (Figure 5):
- a boat-mounted survey for the subtidal area (Figure 6)
- measurement of water levels at six locations throughout the estuary
- measurement of currrent flows, and suspended sediment concentrations at three locations within the estuary
- numerical modelling of the tidal flows before and after breaching (for a number of different scenarios)

4.2 FLOW MODEL DESCRIPTION AND CALIBRATION

The flow model used for the EA Salcott Creek study was a TELEMAC-2D model (See Appendix 1). The grid is shown in Figure 7. The grid resolution varied between 1m and 10m resolution across the saltmarsh (the major concern in this case being the resolution of the various breaches). The model bathymetry is shown in Figure 8. Note that the full bathymetry of the setback fields is represented in the model, even for the baseline condition, (to ensure the pre and post-realignment grids are identical).

The calibration for the spring tide results is shown in Figures 9 and 10. At sites 2 and 5 it can be seen that the observed currents drop rapidly as the water levels fall below that of the sensors. This aside, the calibration shows that the model reproduces the tidal currents well. The neap tide results were similarly well represented but are not relevant for the present study and so are not presented here.

4.3 MODIFICATION OF MODEL FOR THE PURPOSES OF THIS STUDY

For the purpose of the present study representation of the setback fields are not required in the model. Moreover the grid resolution of the EA study model was considered too variable to be used as a basis for evaluating the different degrees of sub-grid resolution. For these reasons the EA model was modified to give the model grid shown in Figure 11. This model had a grid resolution of 3-6m in the saltmarsh areas and of approximately 20m elsewhere and the setback fields were removed from the grid. In all other respects this model was identical to that of the EA model. No further calibration was undertaken.

4.4 TEST OBJECTIVE

The modified model (henceforth known as the “observation” or as simulation 1), which used a very fine grid over the saltmarsh area, was assumed to be “as close as possible” to the observations and to represent a “best” approximation of the estuary system. By reducing the grid resolution (to 20m and 40m) over the saltmarsh areas of the estuary

the accuracy of the model would reduce, which could be measured by comparing the coarser models with the "observation". The objective of the test was to implement the sub-grid technique described in Chapter 3 to see whether this technique reduced the errors in the model prediction associated with the coarse resolution.

Note that the model grid in the main part of the channel was kept constant. In practice near the interface between the channel and the saltmarsh there was some alteration to the grid resolution but this is judged to be a fairly minor effect.

5. Results

5.1 INTRODUCTION

In all fifteen different model simulations of tidal flow were undertaken. The list of runs is given in Table 1. The simulations listed in the Table were chosen to investigate the following effects:

- The effect of deepening the bathymetry to the locally deepest depth (Simulation 7)
- The effect of using the method but with a constant porosity (Simulations 8 and 10)
- The effect of the method on differing resolutions (Simulations 3-5, 11-13 and 15)
- The effect of altering of search radius (Simulations 3-5 and 11-13)
- The effect of lowering the lower limit of porosity (Simulation 6)
- The effect of using a different data source, ie Admiralty Chart data instead of LiDAR, (Simulation 14).

As noted in Section 4.4, Simulation 1 was used as the "observation" or objective standard against which all other simulations would be compared. Simulations 2 and 9 were the respective "baseline" simulations – ie simulations without any subgrid enhancement. These simulations provided a basis to judge the effectiveness of the proposed method.

The predictions of water level and tidal current speed for simulations 2 to 14 are compared to the baseline (simulation 1) at the four locations shown in Figure 12. The locations vary between the main channel of the creek and the saltmarsh itself. The variation between model simulations for the main channel would not be expected to be significant although with increasing proximity to the saltmarsh it is expected that the variation between model simulations would be greater.

Figure 13 shows how the representation of saltmarsh bathymetry within the model deteriorates with increasing resolution. The bathymetry across the transect AB is shown for each of the 3-6m resolution, 20m resolution and 40m resolution "standard" (ie without the method) model grids. It can be seen that,except for the larger channel in the middle of the transect the order of small-scale bathymetric variation is around 1m and that as the grid becomes coarser the bathymetry becomes increasingly smooth and level.

Table 1 Model simulations undertaken during this study

Simulation	Description
1	**"Observation",** 3-6m grid resolution, no sub-grid resolution
2	**"Baseline",** 20m grid resolution, no sub-grid variation
3	20m grid resolution, sub-grid variation, value of porosity, η , constrained to be greater than 0.5, search radius of 4.5m
4	20m grid resolution, sub-grid variation, value of porosity, η , constrained to be greater than 0.5, search radius of 7m
5	20m grid resolution, sub-grid variation, value of porosity, η , constrained to be greater than 0.5, search radius of 10m
6	20m grid resolution, sub-grid variation, value of porosity, η , constrained to be greater than 0.1, search radius of 10m
7	20m grid resolution, bathymetry is given by the deepest point within 4.5m.
8	20m grid resolution, sub-grid variation, value of porosity, η , constrained to be equal to 0.5, search radius of 4.5m
9	**"Baseline",** 40m grid resolution, no sub-grid variation
10	40m grid resolution, sub-grid variation, value of porosity, η , constrained to be equal to 0.5, search radius of 4.5m
11	40m grid resolution, sub-grid variation, value of porosity, η , constrained to be greater than 0.5, search radius of 4.5m
12	40m grid resolution, sub-grid variation, value of porosity, η , constrained to be greater than 0.5, search radius of 12m
13	40m grid resolution, sub-grid variation, value of porosity, η , constrained to be greater than 0.5, search radius of 20m
14	40m grid resolution, bathymetry derived using OS maps and Admiralty Charts
15	**"Observation",** 3-6m grid resolution with sub-grid resolution

5.2 COMPARISON OF MODEL SIMULATIONS

Comparisons of the predicted current speeds for the various simulations are shown at the four locations in Salcott Creek and in the form of peak current speeds across the main area of saltmarsh.

5.2.1 Comparison of results on 20m grid

Figures 14 and 15 show a comparison of simulations 1 (fine grid), 2 (straight bathymetry), 4 (method with varying porosity), 7 (bathymetry based on minimum local bed level) and 8 (method with constant porosity of 0.5). The figures show that the saltmarsh exhibits large peaks in current speed near high water with a long ebb period where current speeds tail gradually decline in magnitude. With distance from the salt marsh this characteristic signature becomes less prominent.

The figures show that it is not immediately apparent whether the method improves the accuracy of the flow model which is why the model results are examined using an objective statistical method in Section 5.3. However the following points can be noted:

- On the edge and immediately downstream of the saltmarsh the ebb tide current speeds are not well represented

- The simulation based on minimum local bed level (Simulation 7) produces current speeds that are significantly too high
- Use of deeper bathymetry (with and without the method) results in current peaks which are earlier in the tide on the flood and later in the tide on the ebb
- With the exception of simulation 7 the predicted peak currents around HW are lower in magnitude.

Figures 16 to 18 show the peak currents occurring in simulations 1 (fine grid), 2 (straight bathymetry), 3 (method with varying porosity) respectively. The figures show that the runs with the coarser 20m grid over the intertidal areas keeps most of the features of the finer grid but that the dendritic channel structure in the finer grid over the saltmarsh areas does not appear to be preserved. A comparison of Figures 16 and 17 shows that there is little difference between the peak speeds produced with and without the method but that the method appears to slightly reduce the extent of areas where peak current speeds are less than 0.2m/s.

5.2.2 Comparison of results on 40m grid

Figures 19 and 20 show a comparison of simulations 1 (fine grid) and 9 (straight bathymetry), 10 (method with constant porosity of 0.5), and 11(method with varying porosity). The closeness of fit of these latter simulations to simulation 1 is examined in Section 5.3. The following points can be noted on the basis of Figures 19 and 20:

- The 40m grid simulations predict current speeds significantly lower than those of the fine grid (and the 20m results)
- Use of deeper bathymetry (with and without the method) results in current peaks which are earlier in the tide on the flood and later in the tide on the ebb.

Figure 21 and 22 show the peak currents occurring in simulation 9 (straight bathymetry) and 10 (method with varying porosity) respectively. Comparison with Figure 16 indicates that the coarser 40m grid shows significantly less “connectivity” than the fine grid and that to a small extent the method enhances the connectivity of the coarser grid slightly.

Figures 23 and 24 show a comparison of simulations 1 and 14, the latter corresponding to the model results for intertidal bathymetry derived from OS maps and Admiralty Chart 3741. The figures show that the predicted current speeds for simulation 14 are far in excess of those of the fine grid results. This can be explained by the very different bathymetry represented in the two simulations. It is important to note that Admiralty Charts are designed for navigation purposes and therefore represent the highest levels in the local bathymetry rather than the average levels which are necessary to produce the correct storage. Calculations based on the LIDAR data showed that this results in an a bed level around 0.7m (averaged over all the intertidal area) higher than the mean local bed level. The corresponding storage is therefore reduced to a small fraction of the real value (see Section 5.3).

5.2.3 Use of method with fine grid

Figures 25 and 26 show a comparison of simulations 1 and 15 at the four comparison locations. In spite of the fine grid the method still results in significant difference in the resulting predictions of current speed. In particular the method induces an earlier flood peak, a later ebb peak and a more pronounced decline of higher current speeds on the

long ebb. These features reflect the enhanced flow through the salt marsh at low water levels resulting from an improved representation of the bathymetry.

5.3 STORAGE ASSOCIATED WITH THE DIFFERENT SIMULATIONS

In order to fully comprehend the results presented in Section 5.2 the storage, or tidal volume, associated with each of the model simulations was calculated. The storage calculated was the tidal volume of the creek upstream of easting 599500. The storage associated with each of the simulations is presented in Table 2.

Table 2 shows that the method slightly underestimates the storage (by up to 10%) if the porosity is allowed to vary and the lower limit of porosity is set at 0.5. Note that the storage resulting from the simulation based on Admiralty Chart bathymetry is a small fraction of the real value.

Table 2 Storage associated with each of the simulations

Simulation	Title	Storage	
		m^3	% difference
1	**"Observation"**	1,111,013	-
2	**"Baseline"** 20m intertidal resolution, bathymetry interpolated onto grid as normal	1,074,316	-3%
3	20m intertidal resolution with method, Porosity ≥ 0.5, Search Radius = 4.5m	998,361	-10%
4	20m intertidal resolution with method, Porosity ≥ 0.5, Search Radius = 7m	962,289	-13%
5	20m intertidal resolution with method, Porosity ≥ 0.5, Search Radius = 10m	935,827	-16%
6	20m intertidal resolution with method, Porosity ≥ 0.1, Search Radius = 4.5m	594,392	-46%
7	20m intertidal resolution with bathymetry defined by the locally deepest point	1,361,835	23%
8	20m intertidal resolution with method, Porosity = 0.5, Search Radius = 4.5m	679,272	-39%
9	**"Baseline"** 40m intertidal resolution, bathymetry interpolated onto grid as normal	1,033,572	-7%
10	40m intertidal resolution with method, Porosity = 0.5, Search Radius = 4.5m	651,204	-41%
14	40m intertidal resolution, Bathymetry derived from OS maps and Admiralty Charts	70,533	-94%

5.4 OBJECTIVE COMPARISON OF PREDICTIONS WITH THE FINE GRID RESULT

The comparisons of model results presented in Section 5.2 are informative but by no means present an objective summary of model performance. For this an objective measure is required. This Section presents such an objective test using the Briers Skill Score.

The Briers skill score is used to measure the performance of model predictions against observations. We use the method to compare the accuracy of model predictions using the subgrid against the performance of model prediction without the method. Thus the Briers Skill Score is used to test the null hypothesis that "the subgrid method makes no difference to the accuracy of model prediction".

The Briers skill score, BSS, for comparison of a set of model predictions, Y_i , against a different set of model predictions, B_i , and a set of model observations, X_i , is given by,

$$BSS = 1 - \frac{MSE(Y, X)}{MSE(B, X)}$$

where MSE(Y,X) is the mean square error given by $MSE(Y, X) = \frac{1}{n}\sum_i (Y_i - X_i)^2$.

In this study Y represents the model predictions using the sub-grid method, B represents the model predictions without the subgrid method and X represents the "observations", here approximated by the fine grid results.

The BSS gives a value of 0 if the null hypothesis is correct – i.e. the model improvement (in this case the sub-grid method) is no better than the baseline prediction (in this case the model without the sub-grid approach). The BSS gives a maximum value of 1 if the model improvement is 100% accurate (i.e. Y=X) and a negative score if the model "improvement" is worse than the baseline.

Table 3 shows the Briers skill scores for simulations 3 to 14. The skill scores for the CM20 runs (3-7) use simulation 2 as the baseline. The skill scores for the CM40 simulations (9 to 14) use simulation 9 as the baseline. The "observations" are represented by simulation 1.

Table 3 appears to indicate that the method reduces rather than improves the effectiveness of the flow modelling. The exception to this is the improvement in the representation of flows within the saltmarsh for the 40m resolution results (simulations 11 to 13). However, the nature of the "observation" (simulation 1) against which all of the flow model runs are compared must be considered.

Table 3 Briers Skill Scores for simulations 3 to 13 (using simulation 1 as "observation")

Simulation number	Description	Briers Skill Score				
		Saltmarsh	Saltmarsh Entrance	500m downstream	Channel	Average
3	20m intertidal resolution with method, Porosity ≥ 0.5, Search Radius = 4.5m	-0.75	-0.75	-0.16	-1.28	**-0.74**
4	20m intertidal resolution with method, Porosity ≥ 0.5, Search Radius = 7m	-0.01	-1.08	-0.29	-0.66	**-0.51**
5	20m intertidal resolution with method, Porosity ≥ 0.5, Search Radius = 10m	-0.7	-0.57	-0.43	-1.48	**-0.80**
6	20m intertidal resolution with method, Porosity ≥ 0.1, Search Radius = 4.5m	-2.33	-0.67	-0.24	-2.07	**-1.33**
7	20m intertidal resolution with bathymetry defined by the locally deepest point	-0.1	-1.79	-1.53	-7.2	**-2.66**
10	40m intertidal resolution with method, Porosity = 0.5, Search Radius = 4.5m	0.05	-0.14	-0.13	-1.16	**-0.35**
11	40m intertidal resolution with method, Porosity ≥ 0.5, Search Radius = 4.5m	0.16	0	-0.01	-0.42	**-0.07**
12	40m intertidal resolution with method, Porosity ≥ 0.5, Search Radius = 12m	0.12	-0.12	0.04	-1.53	**-0.37**
13	40m intertidal resolution with method, Porosity ≥ 0.5, Search Radius =20m	0.14	-0.11	-0.84	-2.41	**-0.81**

Figures 24 and 25 show a comparison of simulation 1 and simulation 15 (the same as simulation 1 but with the algorithm implemented also). It can be seen that the impact of the algorithm is itself significant, even for near identical runs with a small search radius. This difference introduces an area of uncertainty inherent to this study. The lack of detailed observations within the saltmarsh means that it is impossible to say for certain which of simulation 1 and simulation 15 more adequately represents the flow throughout the estuarine system. If simulation 1 is a better representation then the method has failed to improve model accuracy for this example of Salcott Creek. However, if simulation 15 is a better representation then it is still possible for the method to improve the model accuracy. This possibility is investigated in Table 4 which repeats the Briers Skill Score analysis of Table 4 but this time using simulation 15 as the "observation" against which all model runs are compared.

Table 4 shows that under the assumption that simulation 15 is a more accurate representation of flow within the system than simulation 1, the method succeeds in improving model accuracy significantly for a given grid resolution. The success of the method is pronounced for the 20m resolution, because the coarser intertidal resolution of 40m intrudes into the channel and gives a poorer prediction of flow in the channel.

As might be expected the improvements resulting from the method are greater within the salt marsh.

Additionally, the results may also suggest (compare simulations 4, 5 and 6 and 11, 12 and 13) that the accuracy of the method is linked to the search radius and that there is an optimum search radius associated with any given grid resolution. This is hardly surprising since the standard deviation of the bathymetry increases with the search radius. Figure 27 shows the variation in "average" standard deviation (calculated by averaging the various standard deviations of bathymetric variation within different search radii from cells across the model grid) for different search radii. For the finite element modelling approach, as used here, we suggest that the search radius needs to around 30% of the grid size. This result can be broadly explained by comparing the area of average grid intertidal element (approximating to an equilateral triangle) with the area of the circle circumscribed by the search radius. These are equal (in an ideal situation) when the search radius is equal to $^{1}/_{2\sqrt{3}}$ times the length of the average element "side".

Table 4 Briers Skill Scores for simulations 3 to 13 (using simulation 15 as "observation")

Run number	Description	Briers Skill Score				
		Saltmarsh	Saltmarsh Entrance	500m downstream	Channel	Average
3	CM20 Algorithm P>=0.1	0.34	-0.23	-0.24	-1.62	**-0.44**
4	CM20 Algorithm P>=0.5, SR = 4.5m	0.53	-0.23	-0.06	0.4	**+0.16**
5	CM20 Algorithm P>=0.5, SR = 7m	0.33	0.19	0.17	0.29	**+0.25**
6	CM20 Algorithm P>=0.5 SR =10m	-0.33	0.01	0.17	0.07	**-0.02**
7	CM20 Deep Bathy	0.7	-0.16	-0.87	-2.14	**-0.62**
10	CM40 Algorithm, P=0.5, SR = 4.5m	0.21	-0.1	-0.09	-0.47	**-0.11**
11	CM40 Algorithm P>=0.5, SR = 4.5m	0.17	0.04	0.02	0.03	**+0.07**
12	CM40 Algorithm P>=0.5, SR = 12m	0.23	-0.06	0.08	-0.66	**-0.10**
13	CM40 Algorithm P>=0.5, SR = 20m	0.26	-0.09	-0.8	-1.42	**-0.51**

5.5 INCREASE IN RUNTIMES ASSOCIATED WITH THE METHOD

The effectiveness of the proposed method must be examined both in terms of the increase in accuracy resulting from the method (see Section 5.4) and in terms of the increase in computer time associated with the method. To be effective the method is required to cause increases in run time which are significantly less than the corresponding increases in run time arising from simply increasing the resolution of the model grid.

Without the method the flow model run times were as follows:

Table 5 Observed model run times (without method)

Intertidal resolution	Total number of model nodes in model	Run Time[1] (approx.)
3-6m	37378	6 days
20m	8656	18 hours
40m	6557	12 hours

[1] The run times above correspond to simulations on a SUN SPARC Ultra 60.

Table 5 shows that the increase in intertidal resolution from 40m to 20m corresponds to an increase in run time of only 50%, while the increase in intertidal resolution from 20m to 3-6m resulted in an eight-fold increase in run time.

The method was found to increase the run times shown above by a factor of 15-25%.

6. Conclusions

The studies described above suggest that the sub-grid methodology will improve the representation of flows both within saltmarsh systems and in estuaries containing such systems. For a given resolution, however, the results of this study suggest that the method can only *partially* overcome the inaccuracy introduced by coarser resolution. It should be noted that these results are derived from only one specific estuary and further use of the method in different environments is recommended.

In the examples given above the best results using the method showed significant improvement for (20m) grid cells 20 times larger (in area) than the "observation" simulation cell. This result matches that of Defina in modelling flow throughout the Venice Lagoon (Defina, 2000). However, for (40m) grid cells around 80 times larger (in area) than the the "observation" simulation cell the best results using the method still improved the model results but the poorer connectivity resulting from this coarser grid reduced the effectiveness of the method.

The method was consistently successful at improving flows within the saltmarsh but was less successful at improving subtidal flows. Moreover, outside of the saltmarsh the improvements in accuracy due to the method varied from significant improvement to significant deterioration in accuracy and no clear pattern could be observed with variation in location. The model results do not clearly confirm that there is an optimum search radius for a given grid resolution, although this appears to be the case for the 20m resolution results with a 7m search radius (Simulation 5).

For the case studied the increase in run time associated with the change from 40m to 20m grid cells was relatively small compared to the increase in accuracy resulting from the increased resolution. For coarser resolutions (the definition of which may vary from model to model) the suggestion is that (in terms of accuracy for a given run time) the method may be less effective than increasing intertidal resolution. At higher resolutions the run times increase rapidly while the corresponding increase in accuracy from the ever-increasing resolution reduces. It is for these situations that the method seems best suited.

Another conclusion arising from the study was the poor results obtained when using bathymetry from sources such as Admiralty Charts and the difference in the resulting model bathymetry compared with LiDAR data. The difference in intertidal storage arising from the different bathymetry data was extremely significant.

An algorithm has been devised (See Appendix 2) showing how the sub-grid methodology can be implemented in computational flow models.

7. References

Chesher T J, Price D M and Southgate H N (1995), MAFF Set Back Experiment Tollesbury Creek, Report on model investigation of breaching scenarios, HR Wallingford SR 413, January 1995.

Defina A. (2000), Two-dimensional shallow flow equations for partially dry areas, Water Resources Research, volume 36, number 11, November 2000.

Hervouet J, Samie R and Moreau B (2000), Modelling urban areas in dam-break flood-wave numerical simulations, International seminar and workshop on rescue actions based on dam-break flood analysis, 1-6 October 2000, Seinäjoki, Finland.

HR Wallingford (1989), Computer modelling of intertidal mudflat areas, Report no. ETSU-TID-4067 prepared by HR Wallingford for the Energy Technology Support Unit of the Department of Energy, October 1989.

HR Wallingford (2001), Sustainable Flood Defences. Monitoring of Retreat and Recharge Sites, Project Number MRD 21110, Abbott's Hall, Numerical Modelling, HR Wallingford EX Report 4367, August 2001.

Sutherland, J. and Soulsby, R.L., (2003). Use of model performance statistics in modelling coastal morphodynamics, Proceedings of the International Conference on Coastal Sediments 2003, CD-ROM Published by World Scientific Publishing Corp. and East Meets West Productions, Corpus Christi, Texas, USA. ISBN 981-238-422-7.

Figures

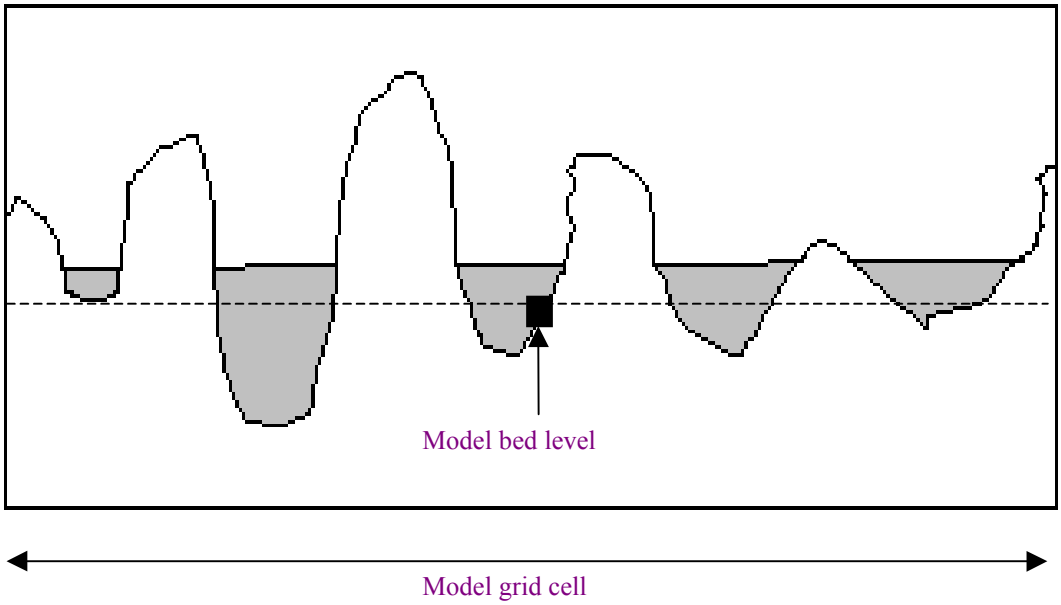

Figure 1 Schematic figure of sub-grid bathymetry

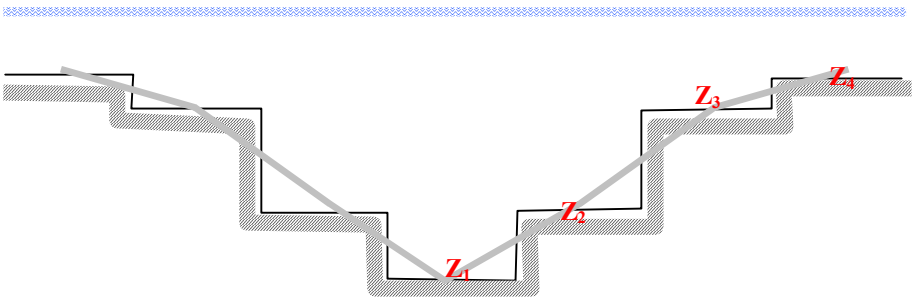

Figure 2 Characterisation of the sub-grid bathymetry

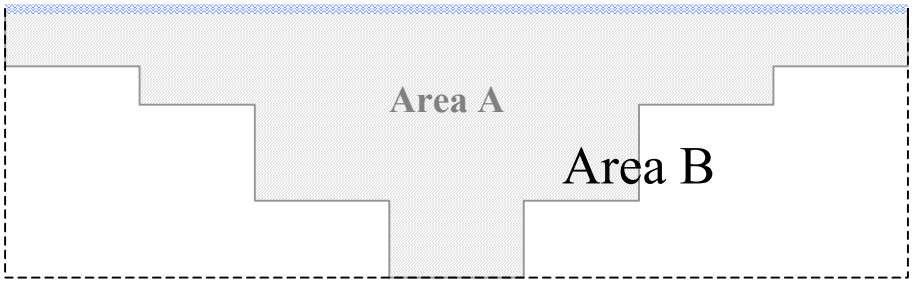

Figure 3 Derivation of areas A and B for calculation of porosity

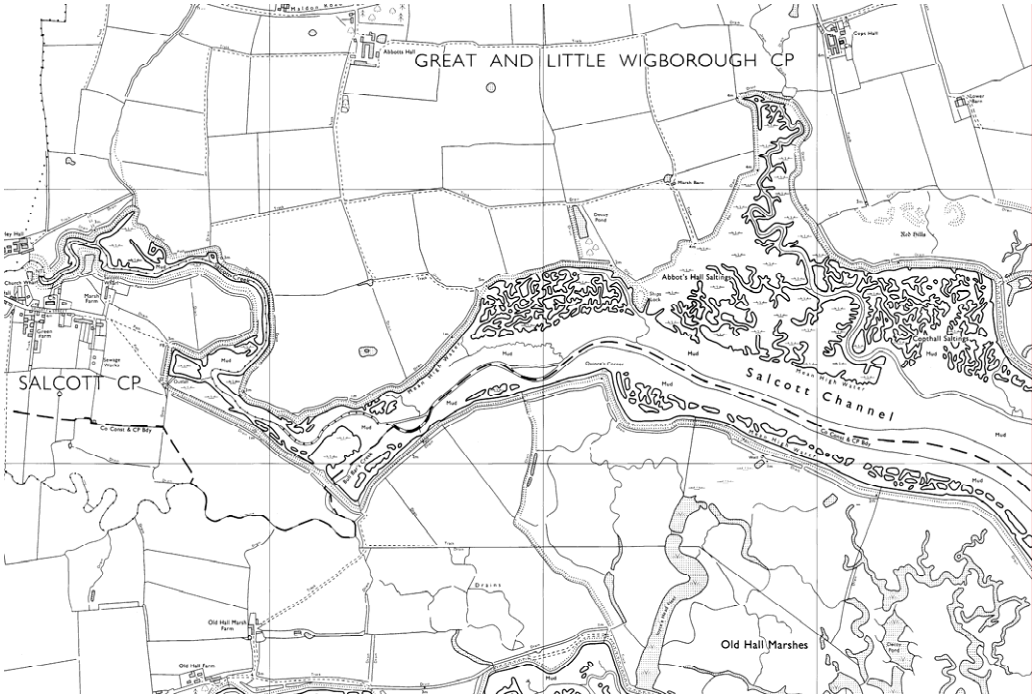

Figure 4 Salcott Creek

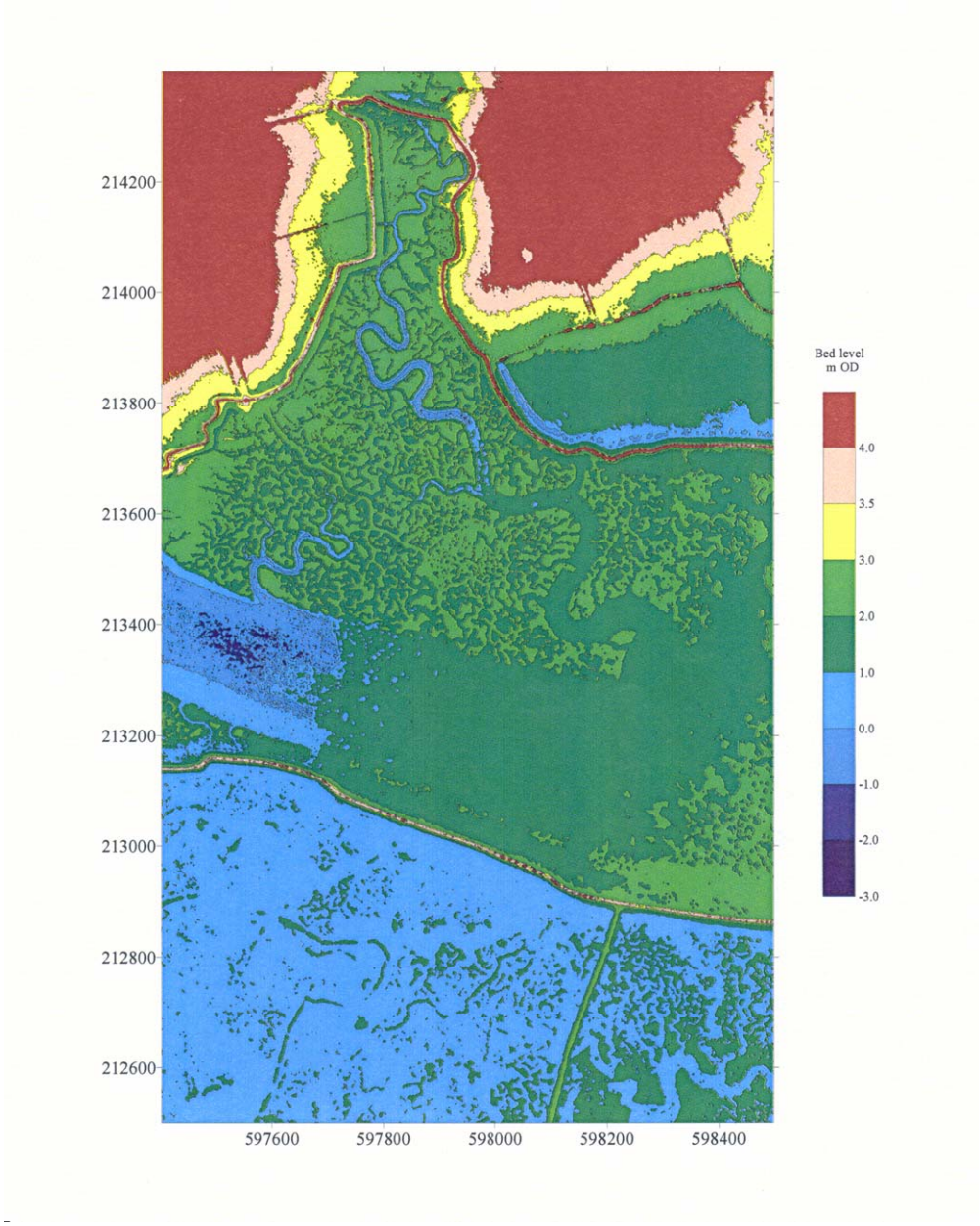

Figure 5 Example of LIDAR data from Salcott Creek

Salcott, Essex

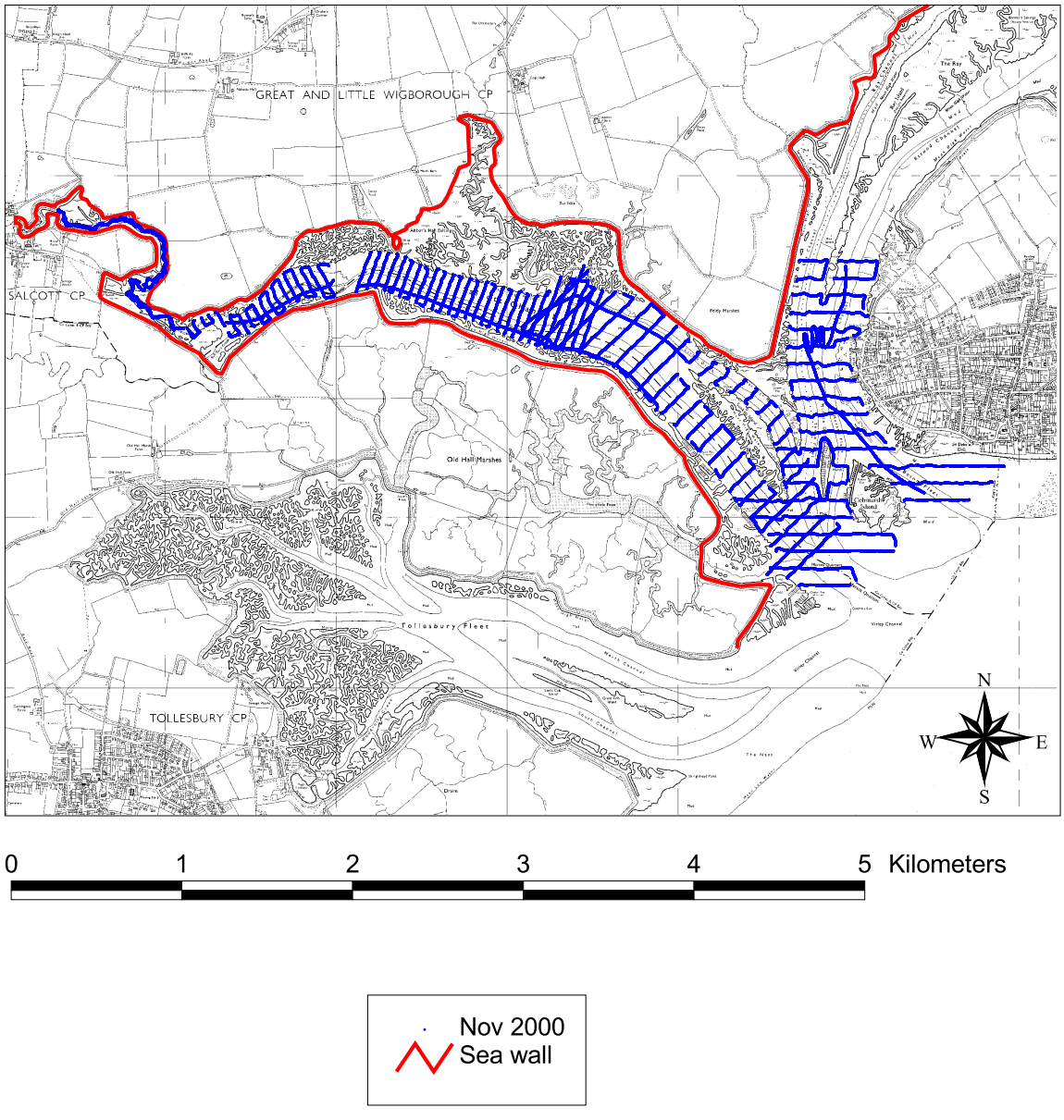

Figure 6 Boat-mounted survey of subtidal area

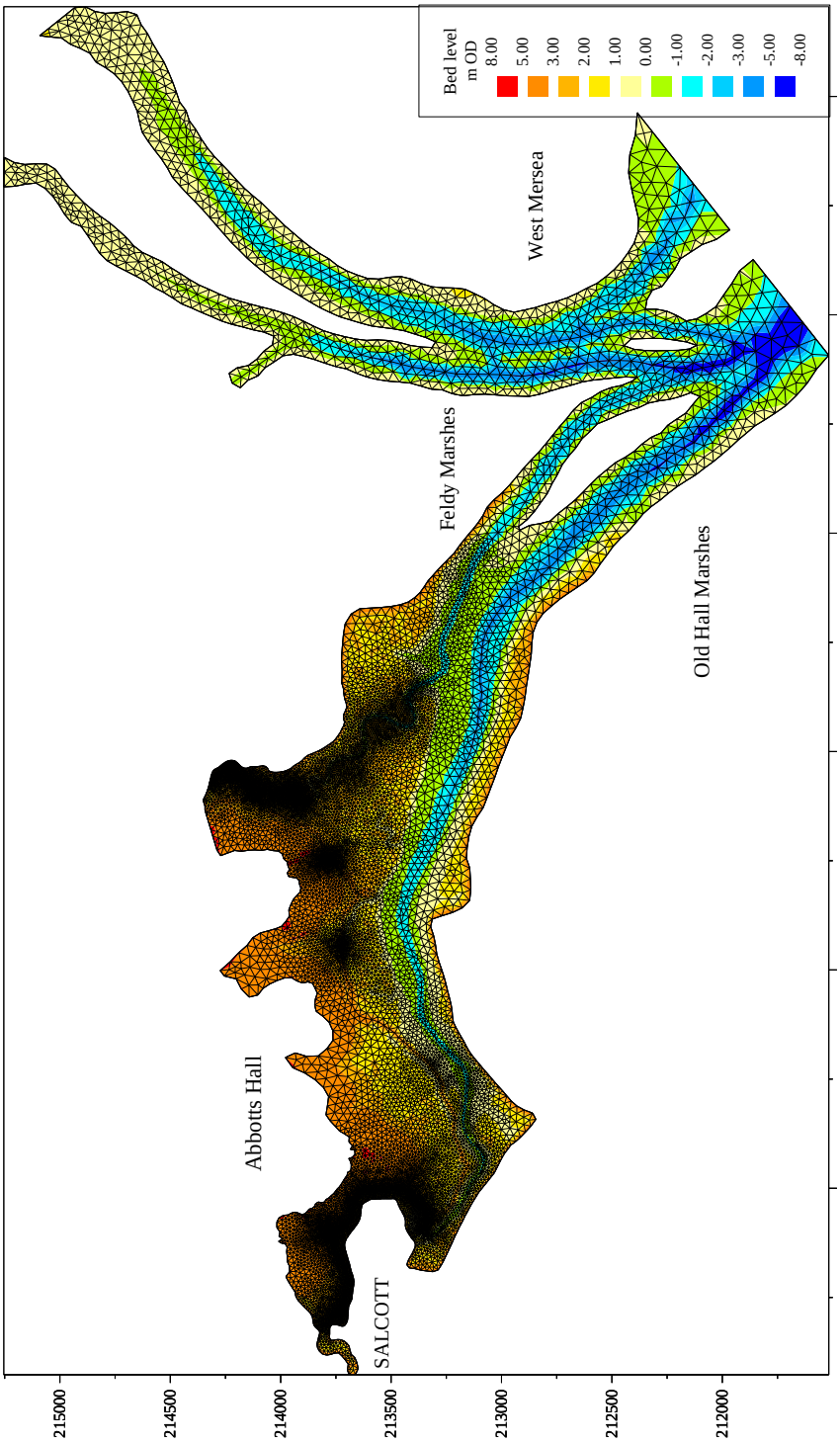

Figure 7 Original study model grid

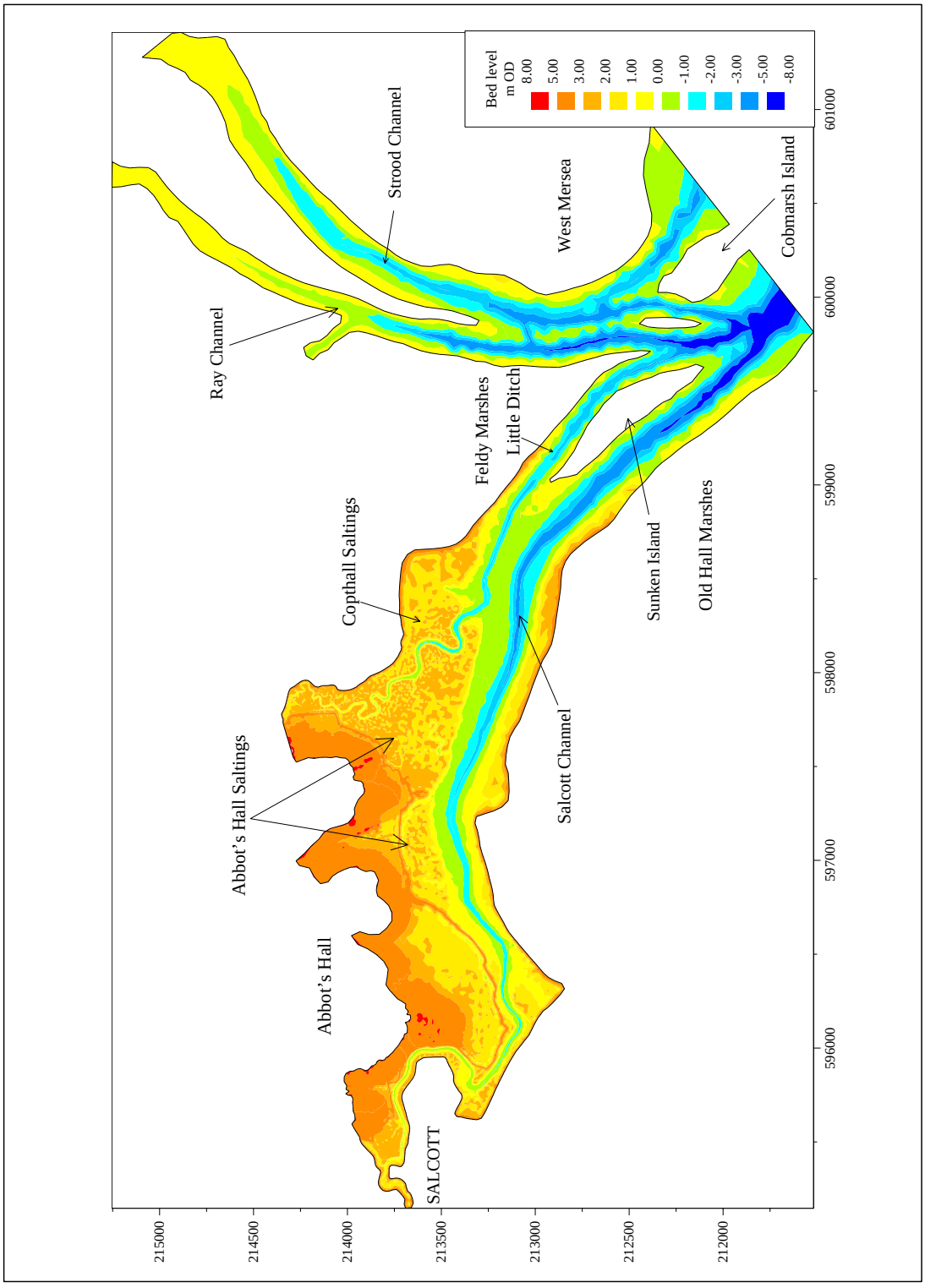

Figure 8 Original study model bathymetry

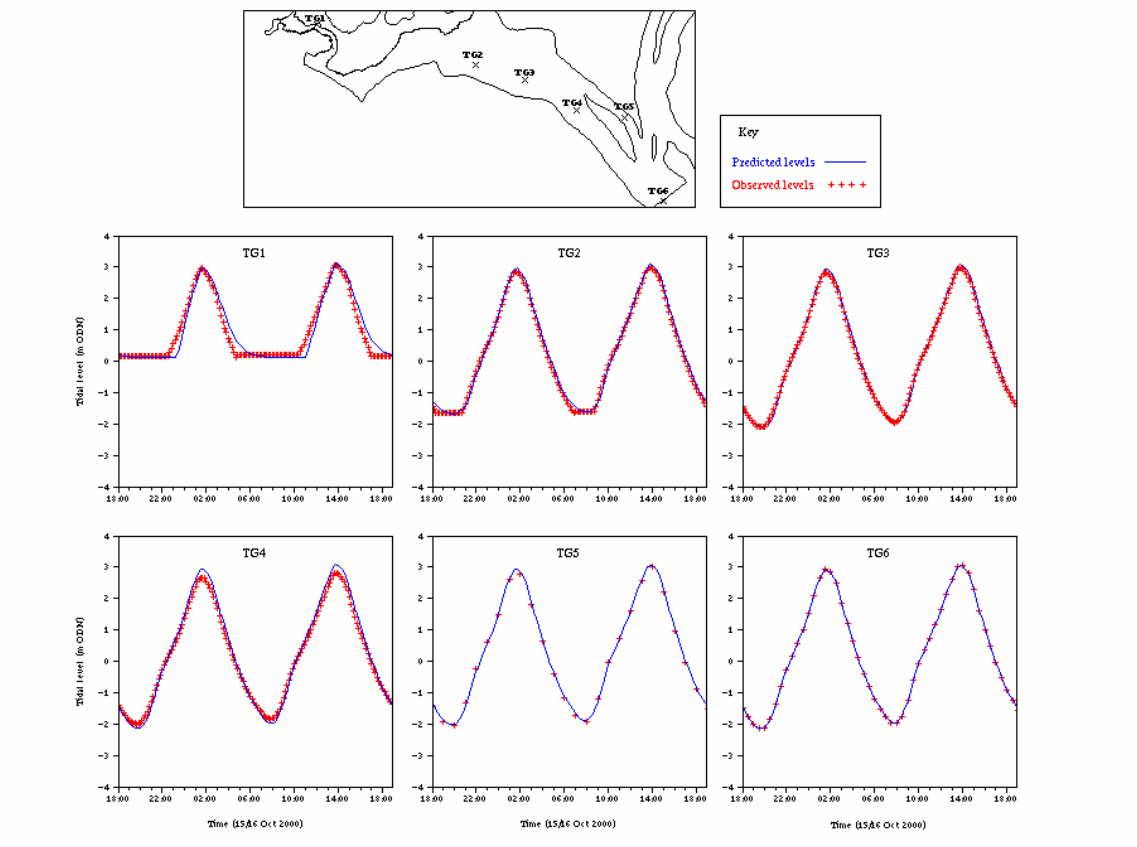

Figure 9 Calibration of water levels

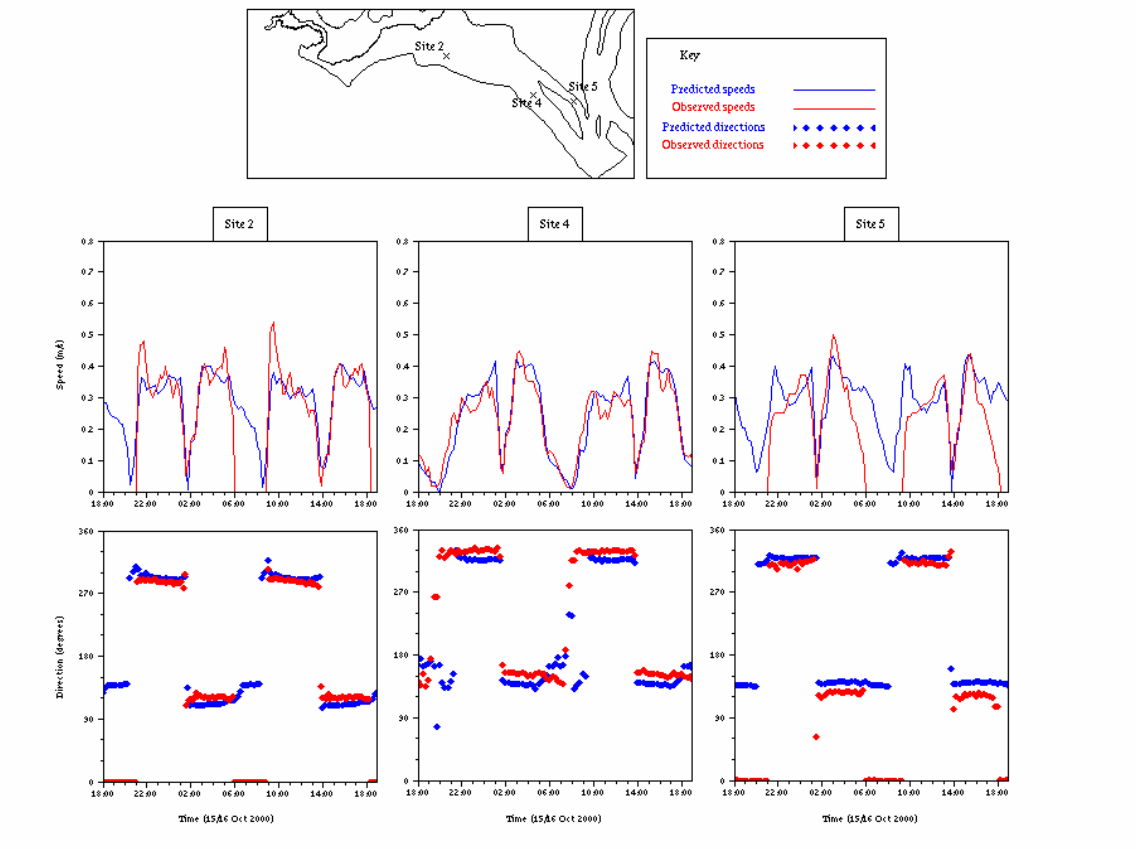

Figure 10 Calibration of current speeds and direction

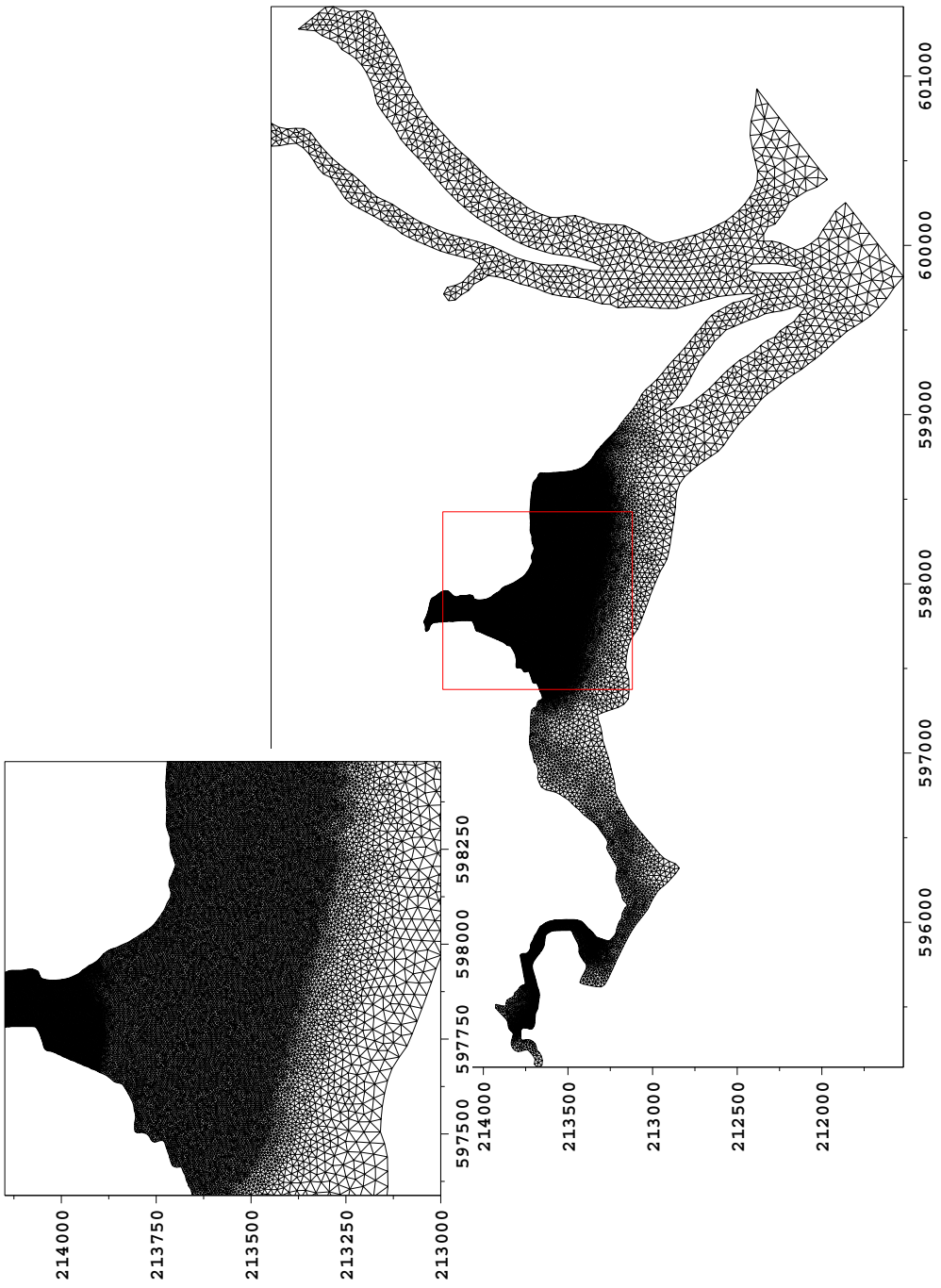

Figure 11 Modified model grid

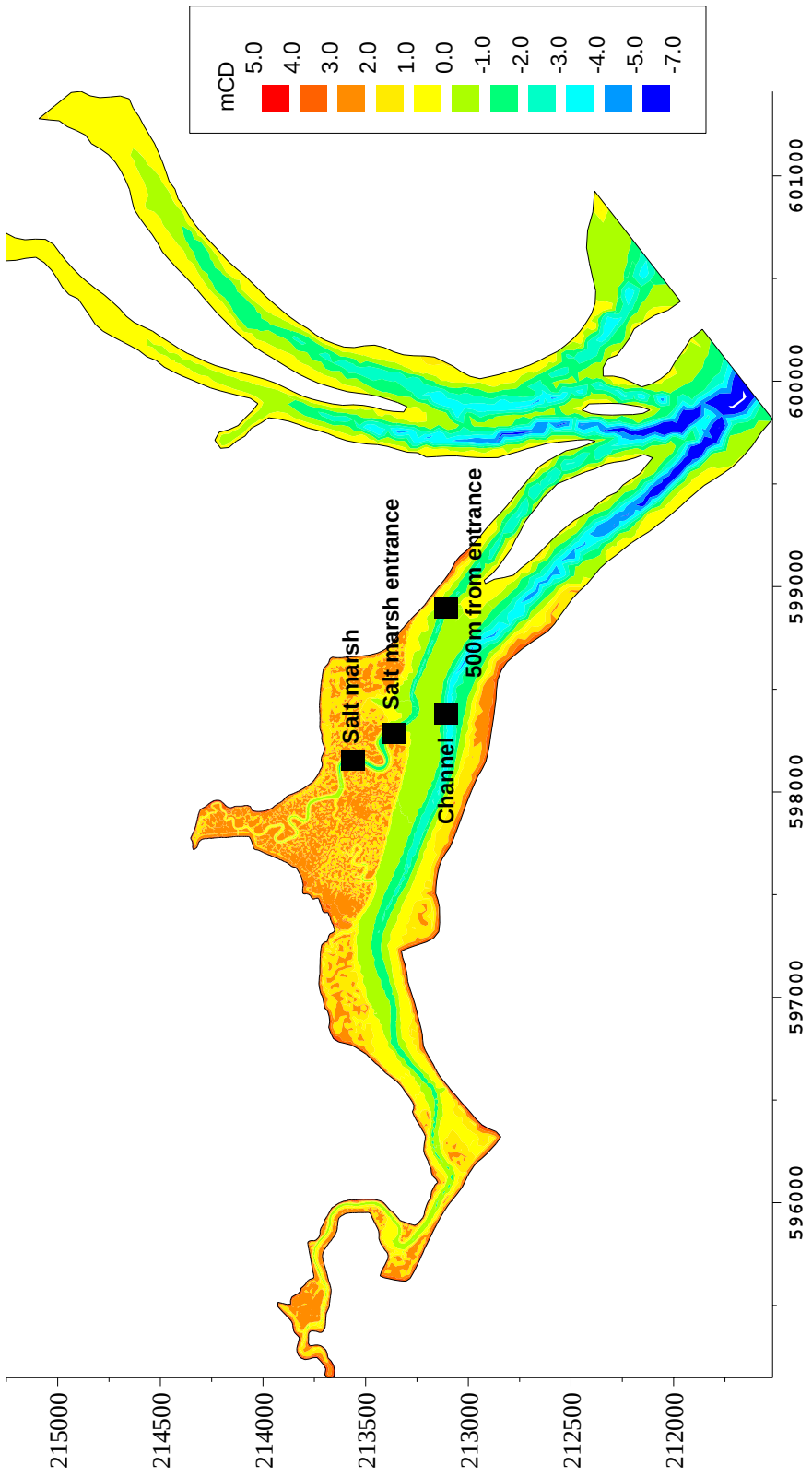

Figure 12 Locations of study comparison points

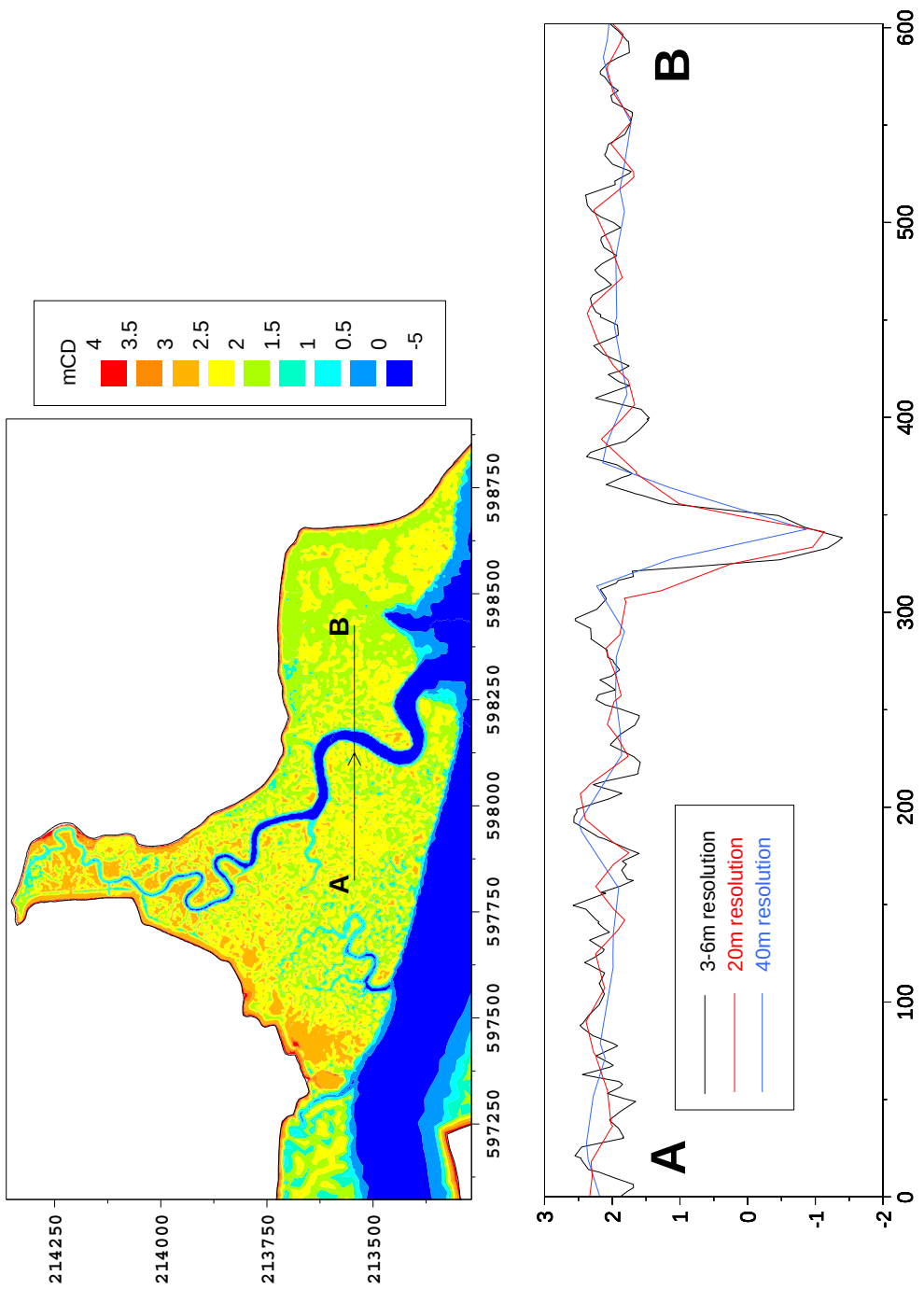

Figure 13 Variation in model bathymetry for 3-6m, 20m and 40m resolution

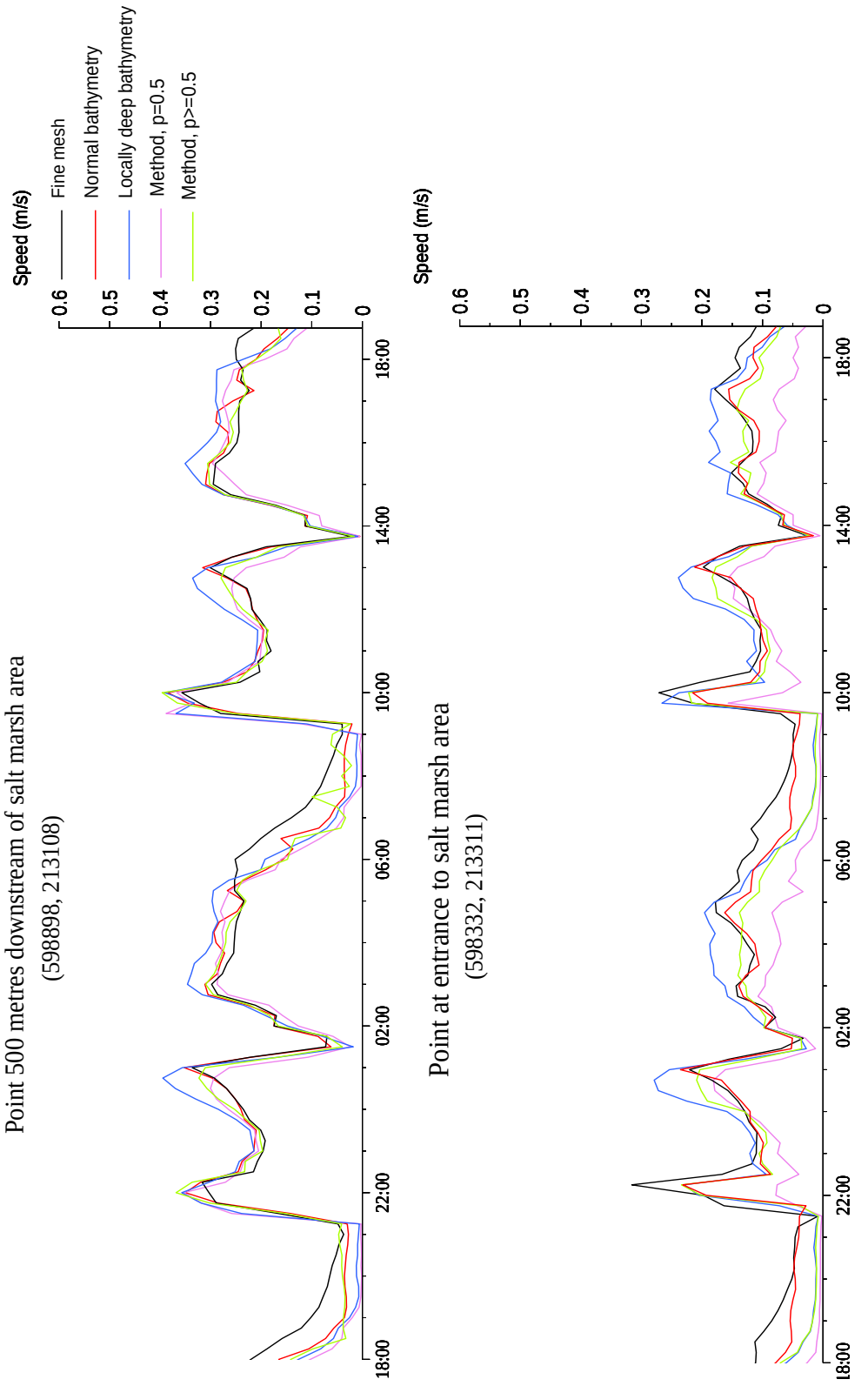

Figure 14 Comparison of predicted current speeds for simulations 1 to 8

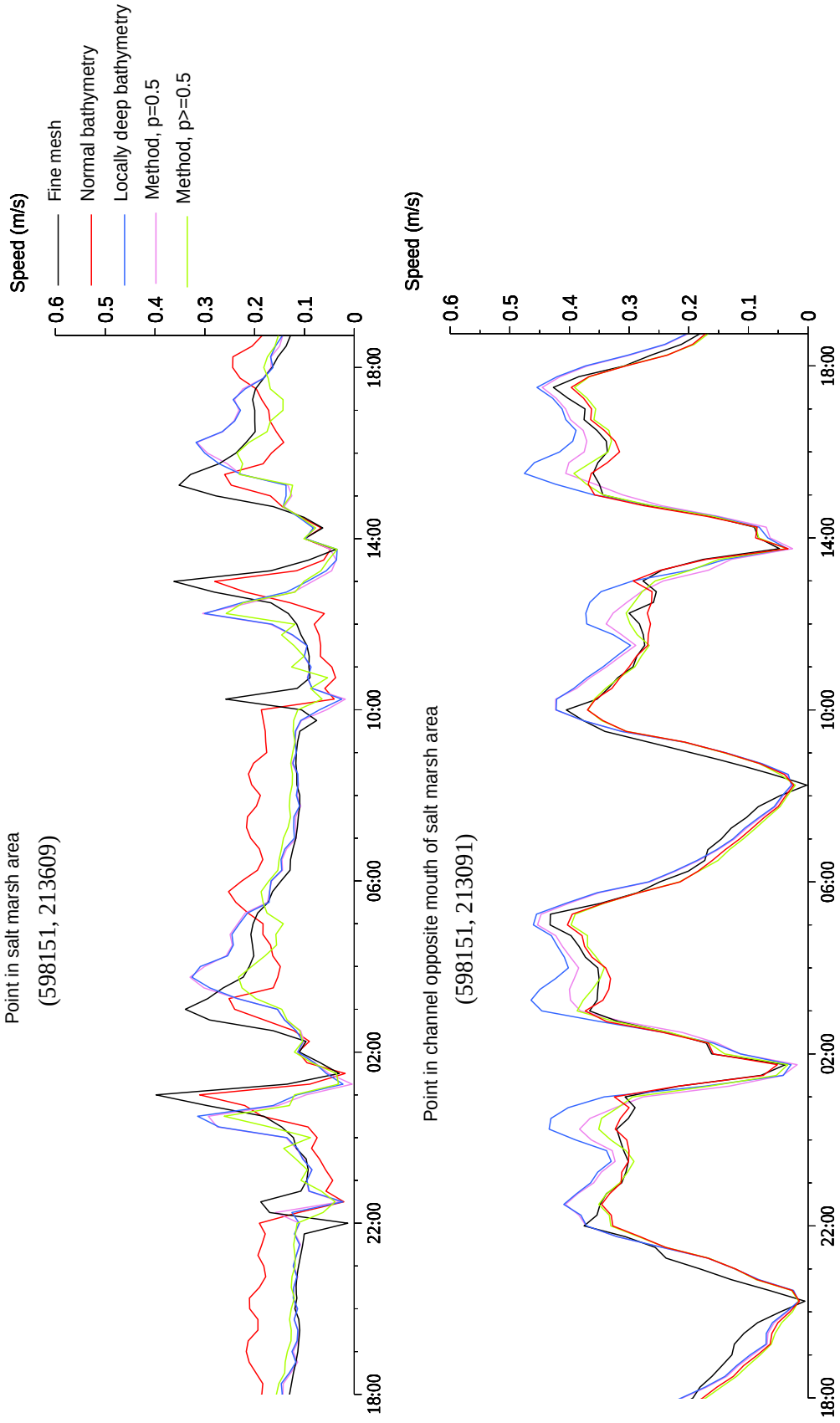

Figure 15 Comparison of predicted current speeds for simulations 1 to 8

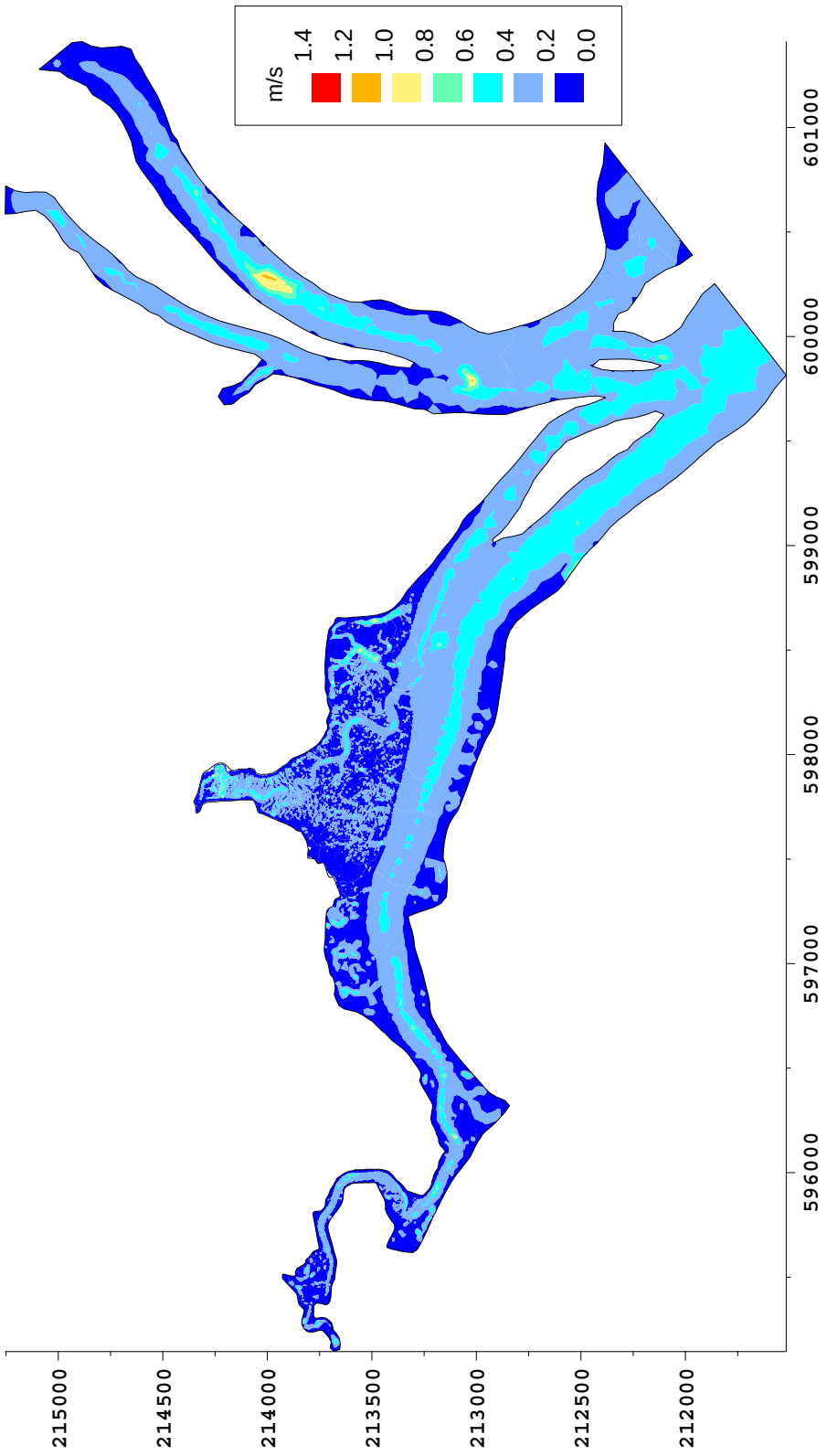

Figure 16 Peak current speeds for simulation 1

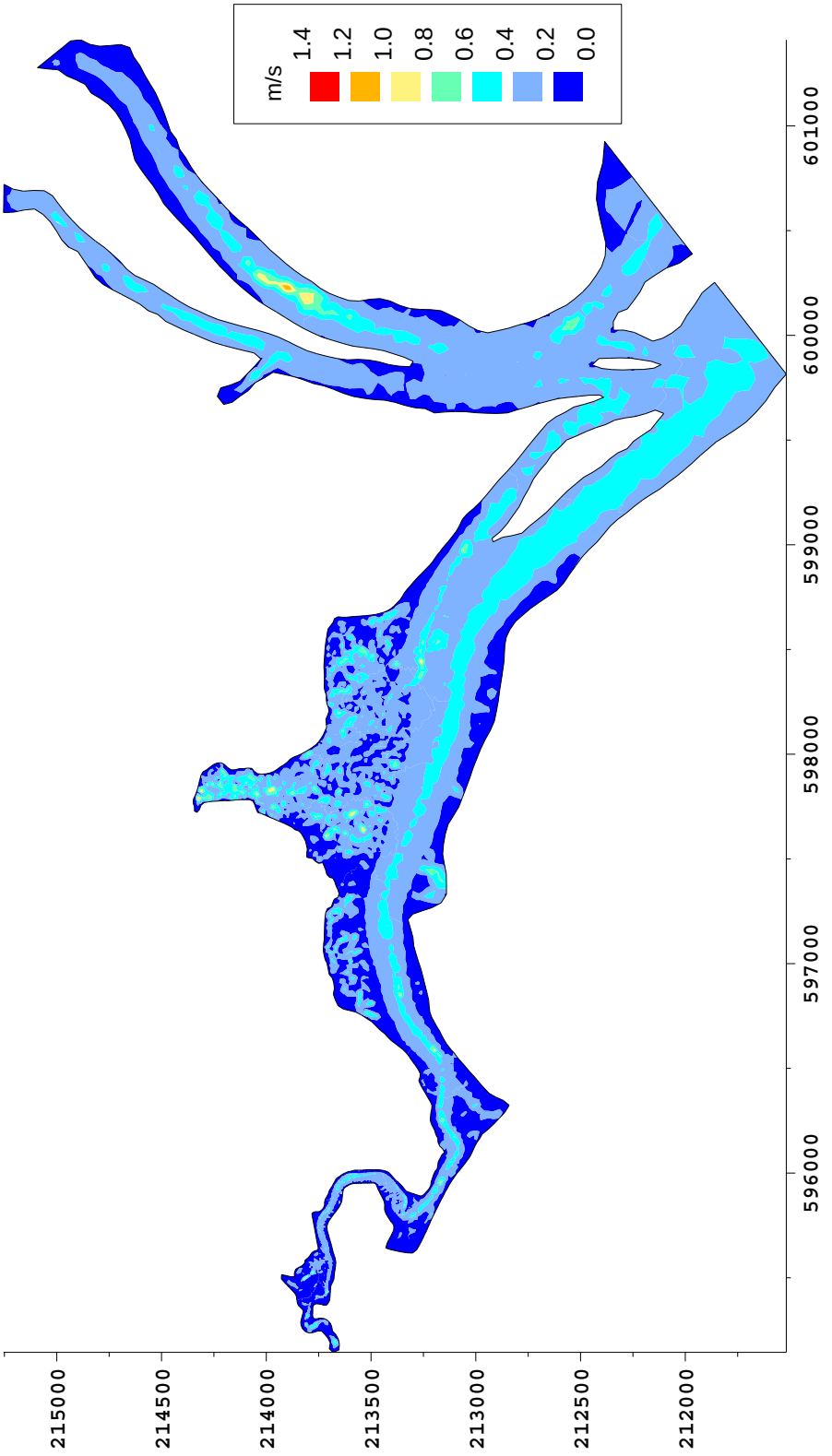

Figure 17 Peak current speeds for simulation 2

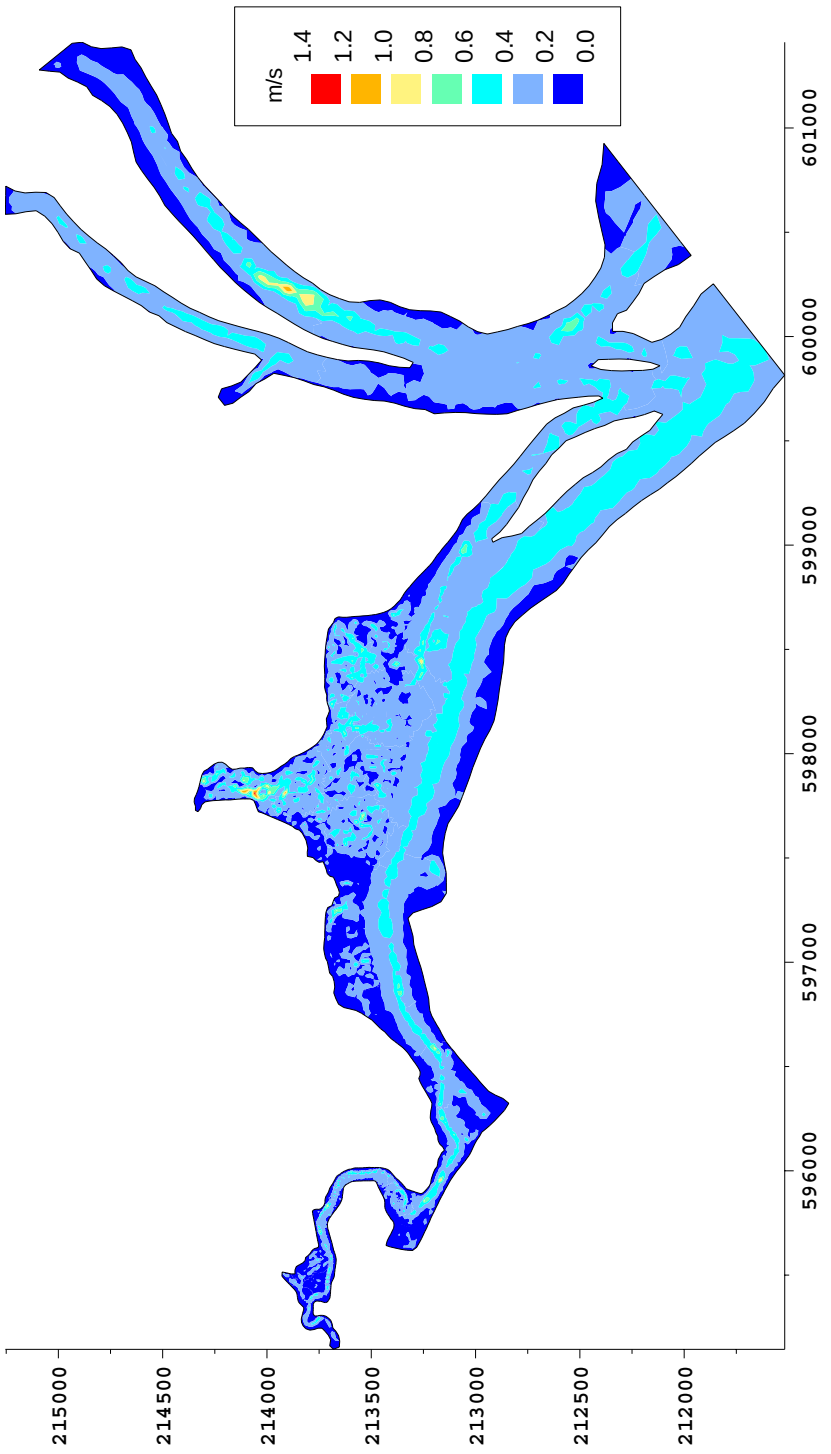

Figure 18 Peak current speeds for simulation 3

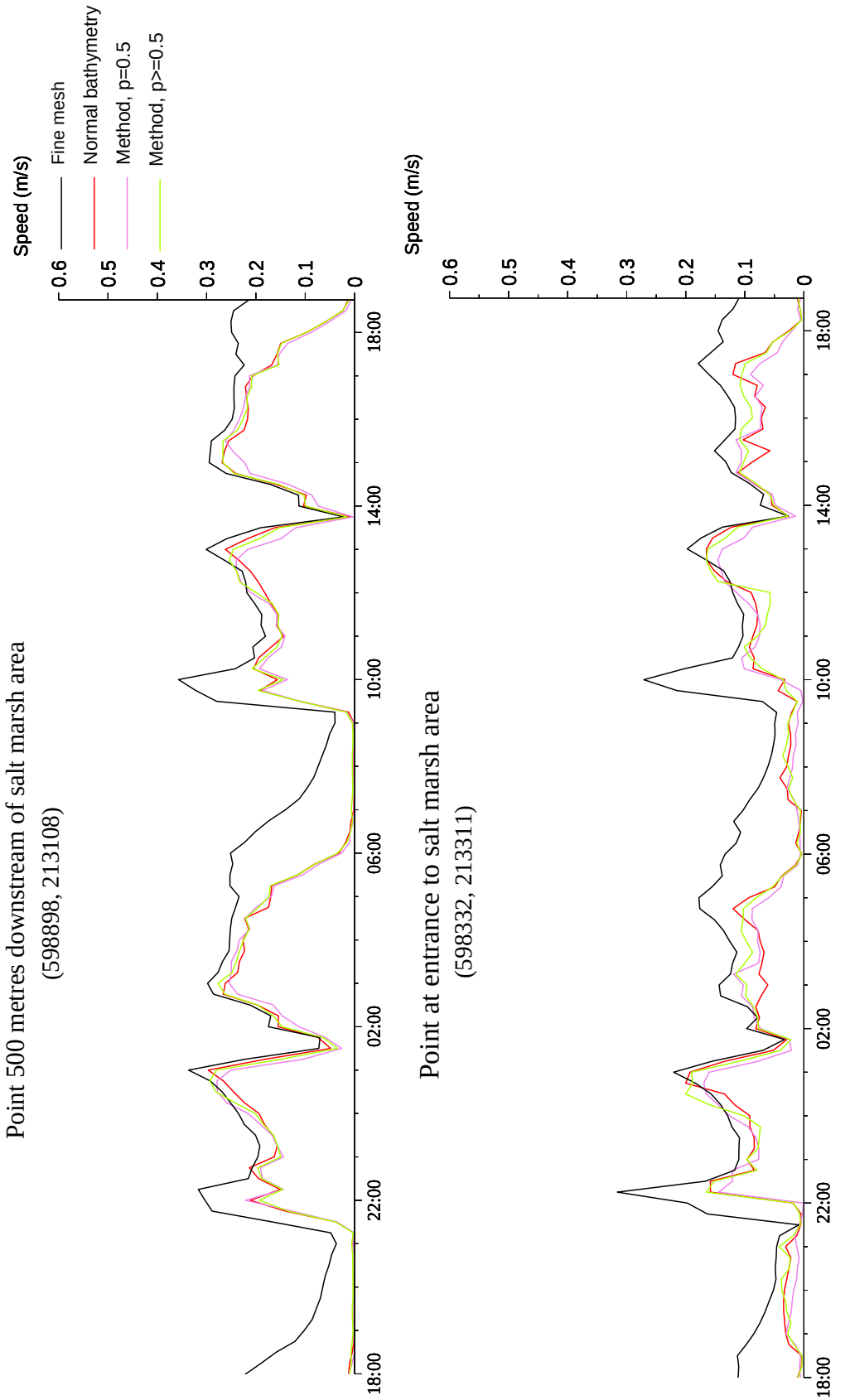

Figure 19 Comparison of predicted current speeds for simulations 1 and 9, 10 and 11

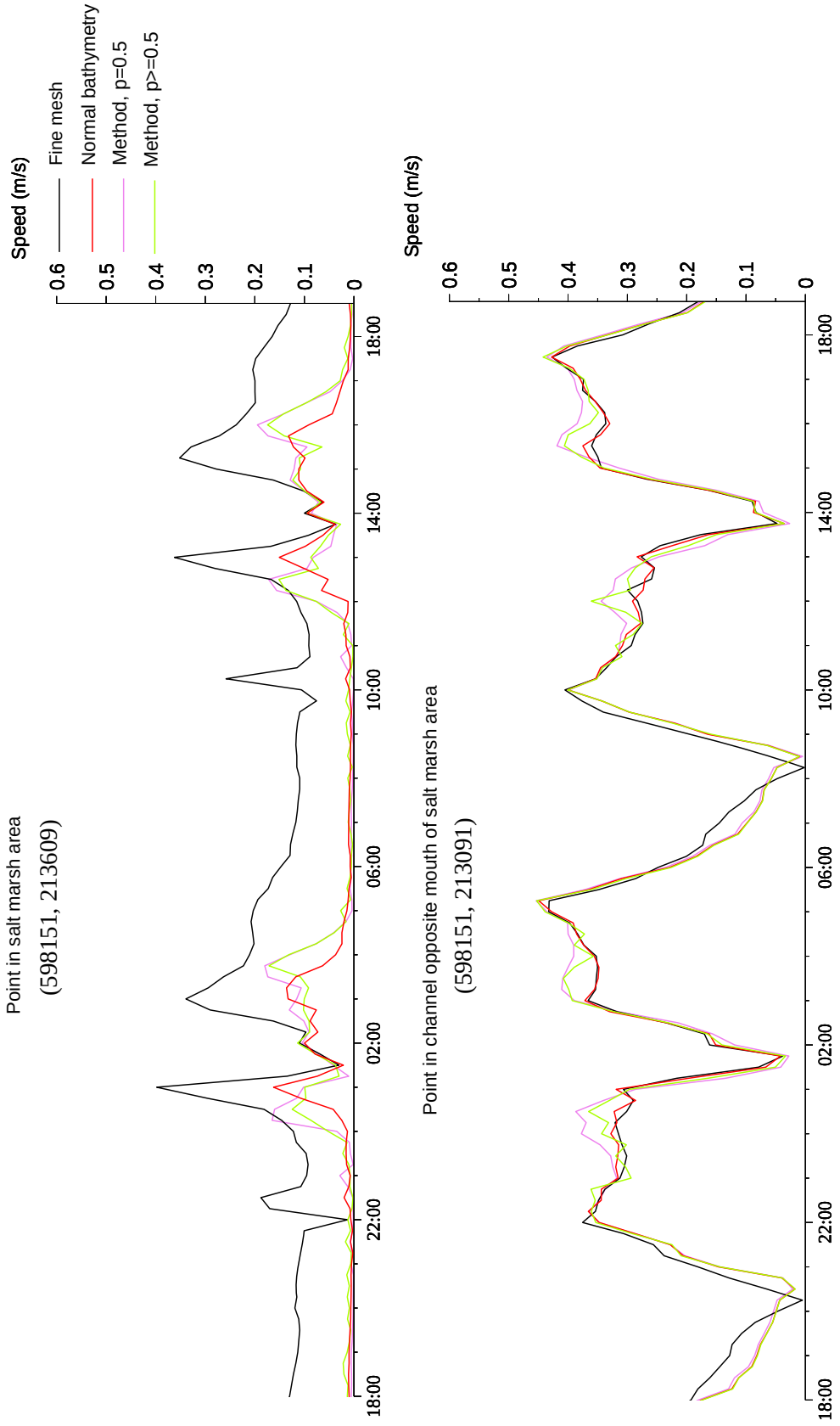

Figure 20 Comparison of predicted current speeds for simulations 1 and 9, 10 and 11

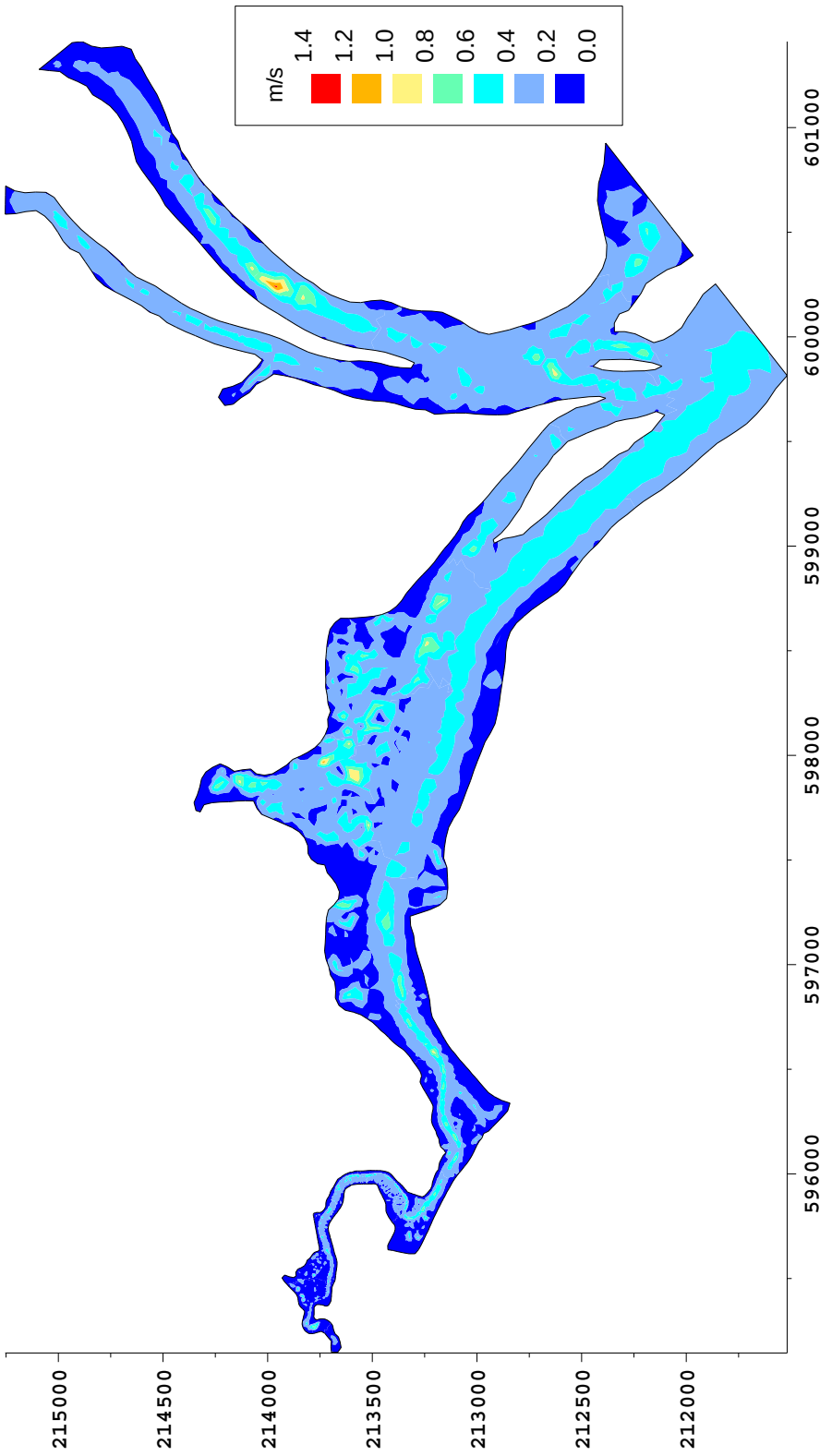

Figure 21 Peak current speeds for simulation 9

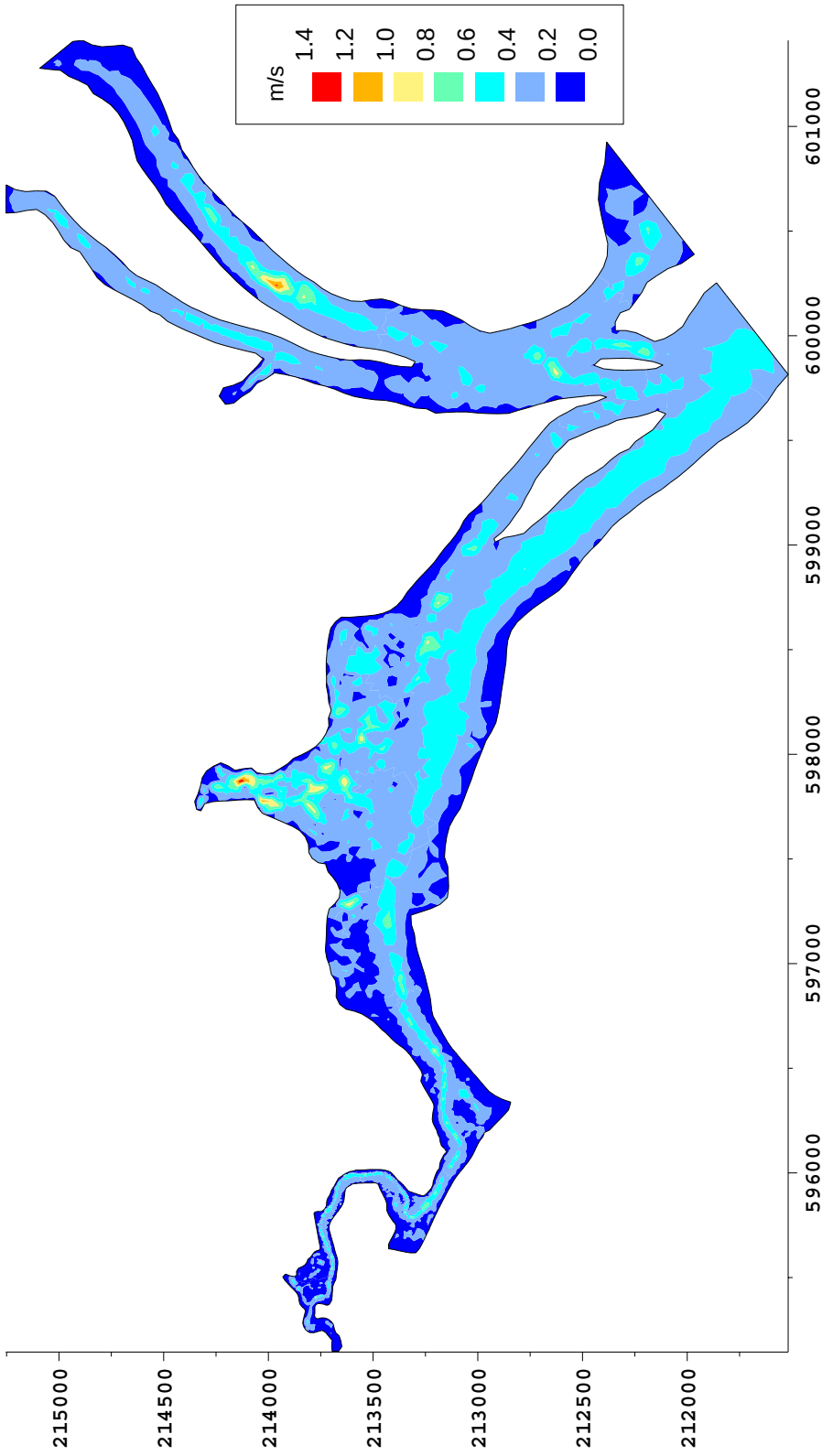

Figure 22 Peak current speeds for simulation 10

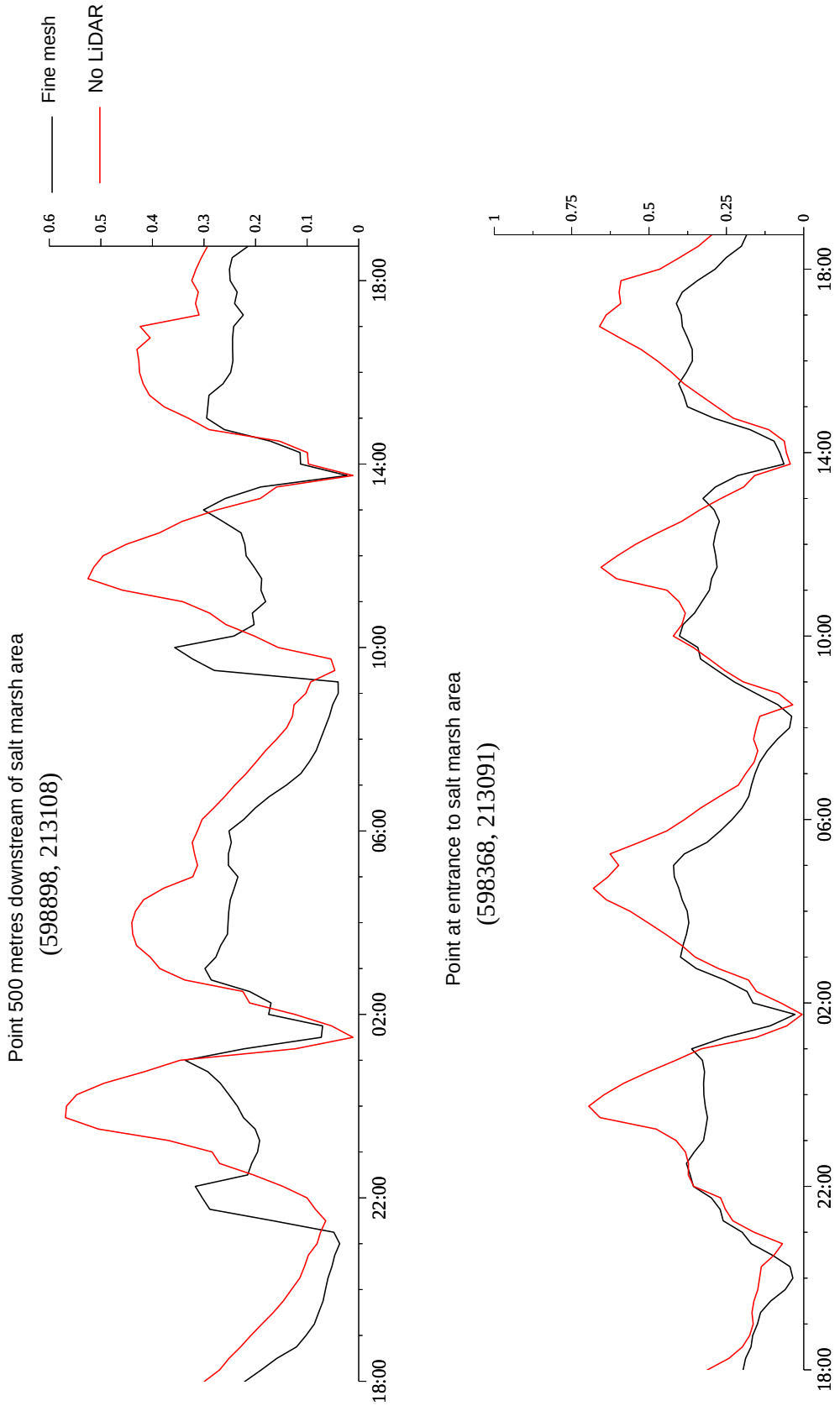

Figure 23 Comparison of predicted current speeds for simulations 1 and 14

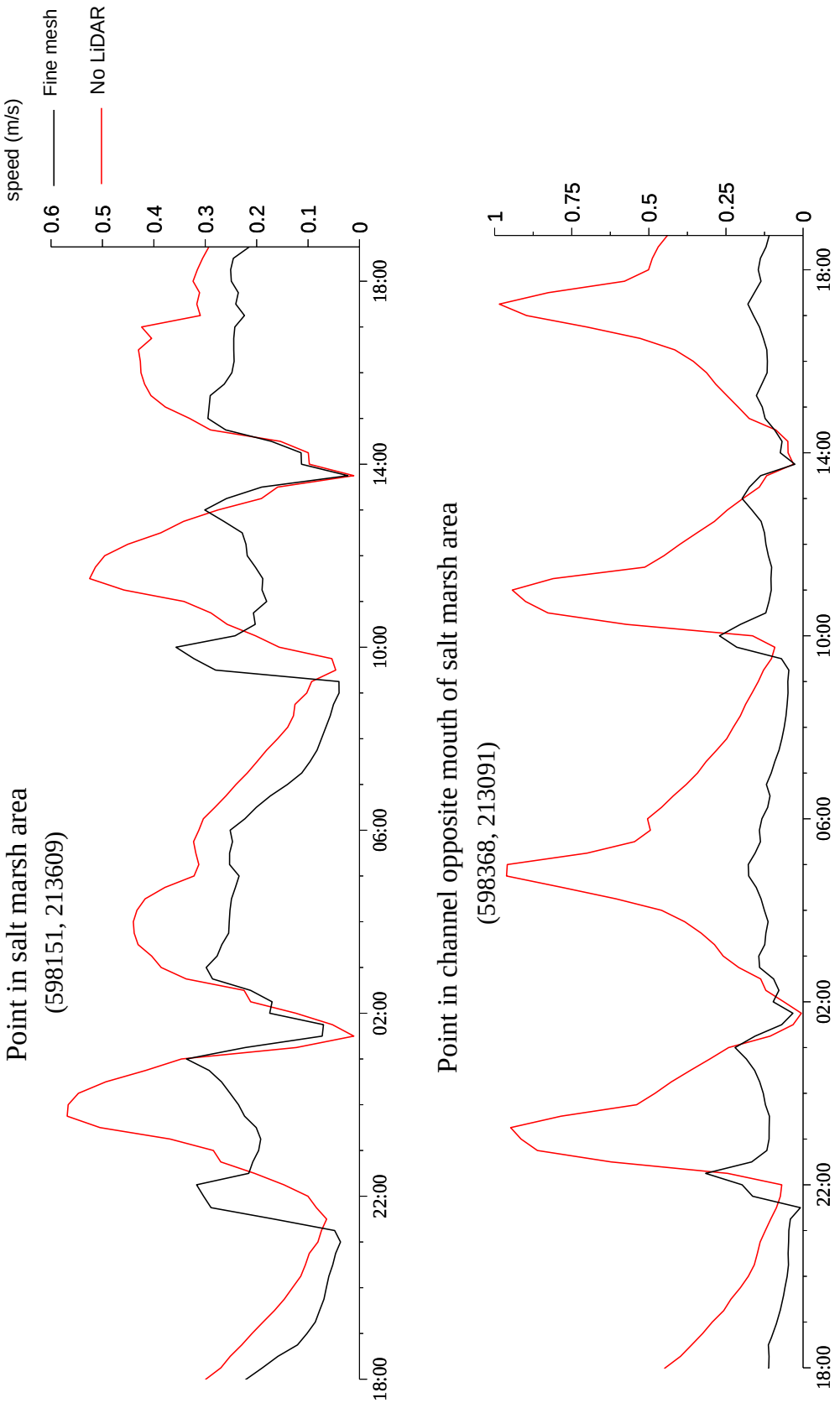

Figure 24 Comparison of predicted current speeds for simulations 1 and 14

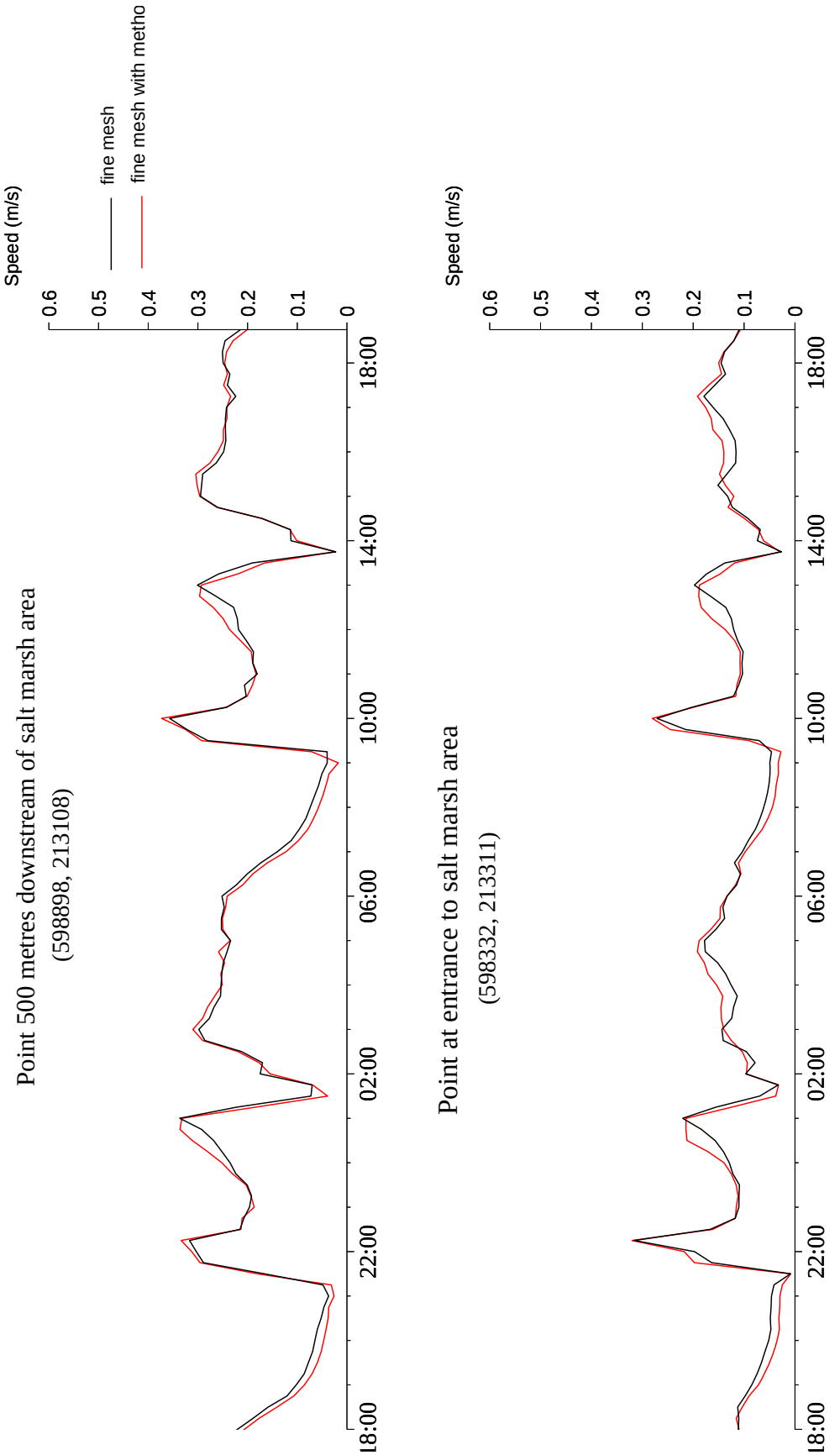

Figure 25 Comparison of predicted current speeds for simulations 1 and 15

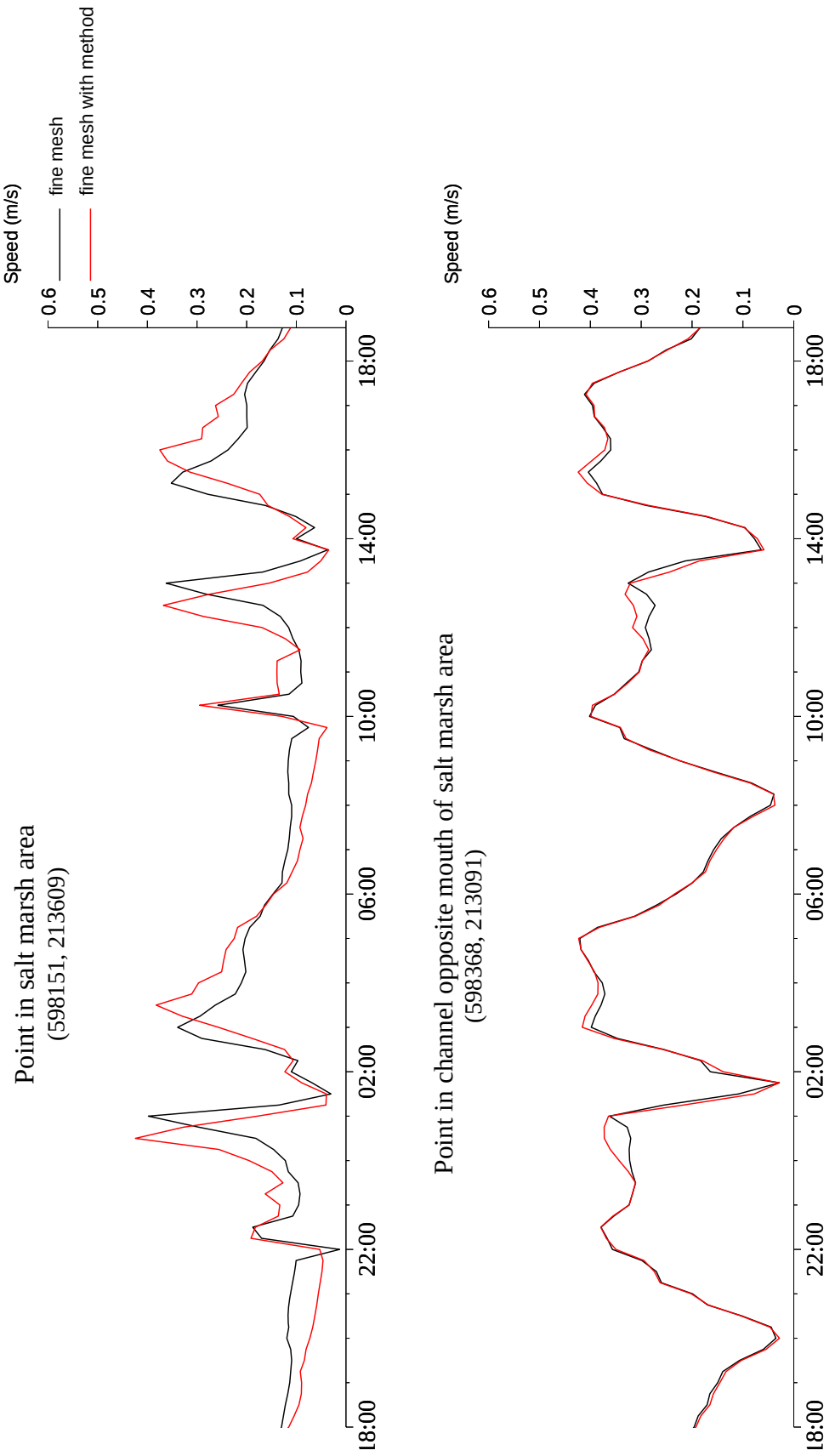

Figure 26 Comparison of predicted current speeds for simulations 1 and 15

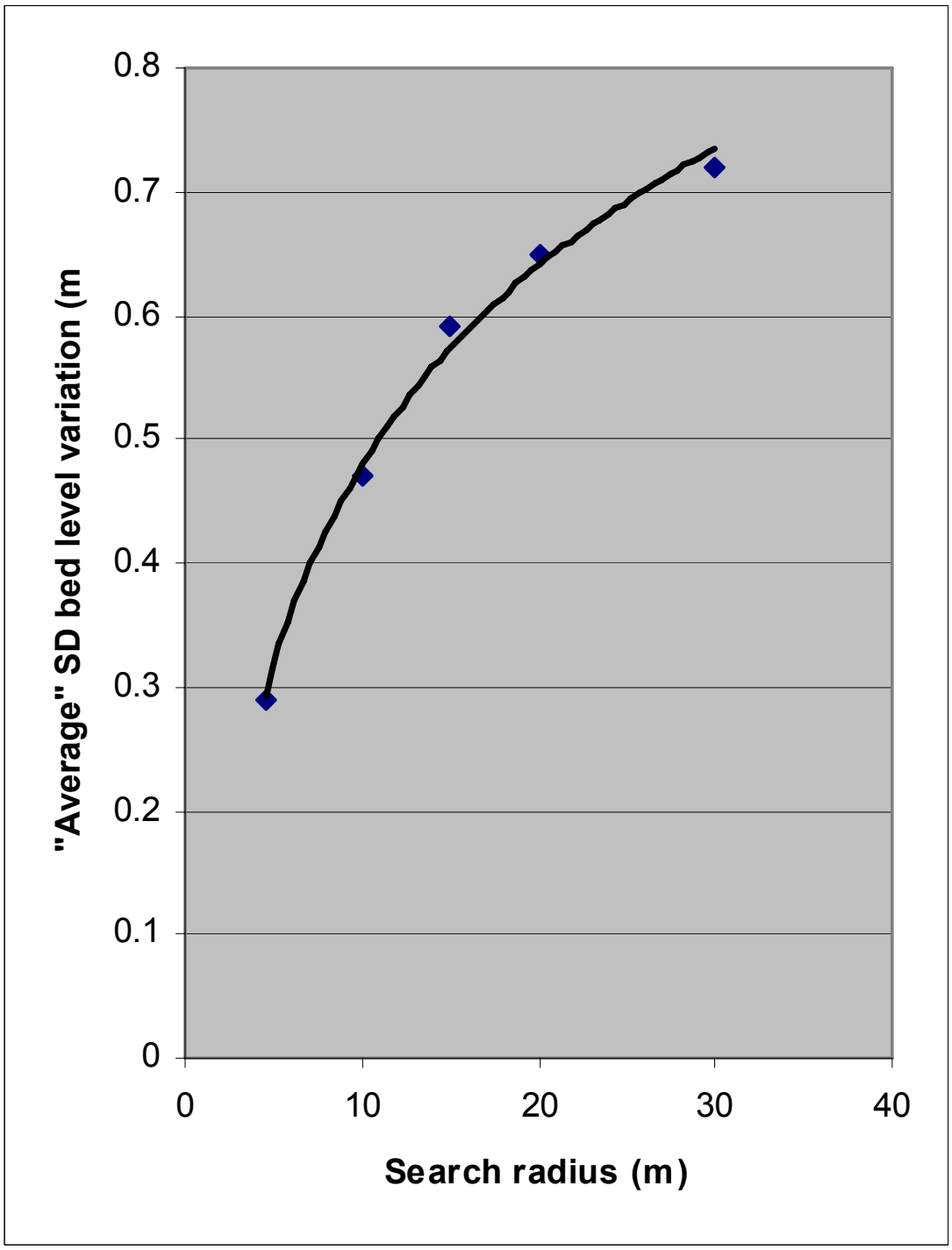

Figure 27 Variation in "average" standard deviation of bathymetry with different search radii

Appendices

Appendix 1 TELEMAC-2D Model Description

Description of model and main areas of application

TELEMAC-2D is a sophisticated flow model, which was originated by LNH in Paris, for free surface flows. It solves the 2D depth-integrated shallow water equations which are used to model flows in rivers, estuaries and seas. It uses finite element techniques so that very flexible unstructured triangular grids can be used. It has been developed under a quality assurance system including the application of a standard set of validation tests.

The model can simulate depth integrated tidal flows in estuaries and seas including the presence of drying banks. It can also simulate flows in rivers including turbulence structures resulting from flow obstructions and transcritical flows. The model has been used with up to 30000 elements.

The advantage of using finite elements lies primarily in the possibility of using a very flexible grid. This is much superior to using an orthogonal curvilinear grid as the user has far more complete control over grid refinement with a finite element system.

The applications of TELEMAC have included studies of ports, coastal management, floods in rivers, cooling water dispersion and infill of navigation channels.

Theoretical background and solution methods

TELEMAC solves the shallow water equations on an unstructured finite element grid (usually with triangular elements). The various variables (bed elevation, water depth, ∇ free surface level u and v velocity components) are defined at the nodes (vertices of triangles) and linear variation of the water and bed elevation and of the velocity within the triangles is assumed.

When the model is used a timestep is chosen and the computation is advanced for the required number of timesteps. There is no particular limit on the timestep for a stable computation but it is best to ensure that the Courant number based on propagation speed is less than about 10. It is found that if the solution is nearly steady then few computational iterations are required at each step to achieve the required level of accuracy, which in TELEMAC is computed according to the actual divergence from the accurate solution. The computation at each timestep is split into two stages, an advective step and a propagation-diffusion step.

The advective step

The advective step is computed using characteristics or streamwise upwind Petrov-Galerkin. The characteristic step makes it possible for the code to handle such problems as flow over a bump giving rise to locally supercritical flow and eddies shedding behind flow obstructions.

The propagation/diffusion step

The finite element method used is based on a Galerkin variational formulation. The resulting equations for the nodal values at each timestep are solved using an iterative method based on pre-conditioned conjugate gradient (pcg) methods so that large problems are solved efficiently. Several pcg solvers are coded and a selection is available to the user. The complete matrix is not assembled, rather an element by

element method is used so that most of the operations are carried out on the element matrices; this is computationally more efficient, both in speed of execution and in memory requirements. Rather than using Gauss quadrature exact analytical formulae are used for the computation of matrices. A symbolic software was used to draw up the formulae used. The software makes it possible to carry out a second iteration of the solution at each timestep in order to represent the nonlinear terms in a time centred way, otherwise these terms are treated explicitly.

Boundary conditions

Boundary conditions are applied at solid boundaries where a zero normal flow and slip or nonslip boundary condition are applied. At open boundaries a selection of possibilities can be invoked depending on whether the flow is subcritical or supercritical or whether a wave absorbing boundary using a Riemann invariant is needed. A water discharge along a boundary segment can also be applied and the software distributes the flow along the segment chosen. This facility is valuable when running models of river reaches and the discharge in a cross section may be known rather than the velocity at each point in the cross-section.

Grid selection

The model can be run with a Cartesian grid for modelling rivers, estuaries and small areas of sea, with the possibility to apply a uniform Coriolis parameter, or on a spherical grid for larger areas of sea in which case the Coriolis parameter is computed from the latitude at each node. The effect of a wind blowing on the water surface and causing a setup or wind induced current or of an atmospheric pressure variation causing an inverted barometer effect can be included, as can a k-epsilon model of turbulence if required.

Friction

The bed friction can be specified via a Chezy, Strickler or linear coefficient, or a Nikuradse roughness length. A variable friction coefficient over the model area is a possibility. Sidewall friction can also be included if wanted. Viscosity can be imposed as a given eddy viscosity value or a k-epsilon model can be used if needed.

Tracer calculation

TELEMAC-2D includes also the capability to simulate the transport of a tracer substance. The tracer is again computed using an advective step followed by a propagation/diffusion step. Tracer boundary conditions can be applied at model inflow boundaries. The tracer calculation has been used in order to simulate cooling water dispersion and mud transport. Sources of water and/or of tracer can be specified in terms of the discharge required and the x and y coordinates of the location.

INPUTS

TELEMAC requires as input a finite element grid of triangles covering the area to be modelled. Bathymetric data from which the bed elevation at each node can be computed is also required covering the area. A file of keyword values is used to steer the computation (supplies bed roughness, timestep, duration of run etc).

Methods of inputting the data

The finite element grid that may be provided by a standard FE grid generator such as I-DEAS or SIMAIL. The software STBTEL (part of the TELEMAC suite) is used to read the output file from the grid generation software. The bathymetry is input using a digitising tablet and the SINUSX software is used to capture the bathymetry data. The data is stored in a form to be read into the TELEMAC system and depths interpolated to the model nodes.

Methods of checking and amending input data

SINUSX is a powerful interactive graphical software that can be used to check and amend the input data. Bathymetric curves can be duplicated, deleted, smoothed, moved etc.

User interface

A steering file editor EDAMOX with online help is available to edit the keyword steering file for TELEMAC. This software can be used to edit the keywords for any part of the TELEMAC system. It can check on the correctness of keyword values supplied. A study manager for TELEMAC is expected at the end of 1994.

Time to setup/calibrate/run/amend model

This depends on the form in which the data is supplied. Typically 1-2 days to digitise the chart data and 1-2 days to create the finite element grid. Boundary conditions may take a day to prepare. A run may take 1 to 5 hours to run a tide (for a 2000 cell model). The duration of the calibration process is hard to generalise as it depends entirely on particular circumstances.

OUTPUTS

Output parameters

The user can select from a range of output parameters including u and v velocity, u and v discharge, water level, bed level, water depth, tracer concentration and Froude number.

Output files

The TELEMAC output is contained in a single binary file which can be input to the graphics post-processor RUBENS. A listing file contains reflection of the input keywords and information on timestep reached, number of iterations to convergence etc. This file can be used to monitor the progress of a run.

Output plots

Results from any part of the TELEMAC system are processed using the interactive graphics system RUBENS. This is a powerful and friendly environment where colour and black and white figures can be produced interactively. By pointing and clicking time history plots, cross sections, vector plots and contour plots of any parameter at any position can be produced. Moreover parameters other than those input can be calculated in RUBENS and plotted.

HARDWARE REQUIREMENTS

TELEMAC is available on UNIX workstations SUN/HP and DEC. RUBENS requires 8Mb of RAM to run but performance is greatly enhanced with 12Mb. RUBENS and SINUSX can be run using either Open Windows or X Windows.

GENERAL

Interaction and compatibility of the model with other models

The main modules apart from TELEMAC-2D itself (the 2D flow model code) are SINUSX and RUBENS (described above).

The TELEMAC suite includes a bed load transport model (TSEF) and a suspended load model (SUBIEF). Also a wave model ARTEMIS that solves the mild slope equation.

The TELEMAC modelling suite also includes a quasi-3D random walk model for pollution transport modelling and a detailed water quality model with many water quality parameters including dissolved oxygen balance and particulates.

Quality Assurance

The software has been developed under the quality assurance procedures required by the French Electricity Industry. This has included the production of an extensive dossier of validation tests.

Validation

Validation tests on TELEMAC include:

Simulation of the eddies produced behind bridge piers. This test case includes the ability of the model to produce an unsteady solution from steady boundary conditions (von Karman vortex street).

Drying on a beach.

Simulation of the tides on the continental shelf including the Bay of Biscay. This model has been closely compared with the observed tides at coastal sites.

Flow over a step in the bed with critical flow and a hydraulic jump. This solution is compared with the analytically known solution to this problem.

Past and current users

Bristol University Agriculture Department
Laboratoire Hydraulique de France
Forth River Purification Board
Franzius Institute
Port Autonome de St Nazaire

Projects where model has been used

Examples of recent projects where TELEMAC has been used at HR Wallingford are:

Location	Client	Date
Port Klang Marine Industrial Park	HICOM-Selangor	Sept 1993
Great Yarmouth Harbour	Great Yarmouth Harbour	May 1994
Southern North Sea	Crown Estate	July 1994
Harwich Harbour	Harwich Harbour Authority	June 1994
Blackwater Estuary	MAFF	May 1994
Dorset coast and the Solent	Poole Borough Council	May 1994
Firth of Forth	Forth River Purification Board	January 1994
Harwich/Felixstowe	Harwich Haven Authority	1995/96
Pipavav, India	Howe Consultants	
Dabhol, India	ENRON	1995
Alderney Harbour, UK	States of Guernsey	1996
Gwadar New Port, Pakistan	Karachi Port Trust	1996

Future developments and timescale for developments

Future developments of the TELEMAC system include TELEMAC-3D, a multilayer shallow water equation model using the same methodology as TELEMAC-2D. Also the TELEMAC study manager. Both are due at the end of 1994.

Appendix 2 Method Algorithm

Aim To improve the accuracy of flow models for estuaries dominated by dendritic systems (saltmarsh and mud flats)

Scientific background
Dendritic systems (which for the sake of this study effectively means saltmarsh and mudflats, although the general principles apply to all such systems) have irregular bathymetry which can vary significantly over length-scales of 1m or less. These small length scales are considerably less than the practically viable scales of 2D flow model grids for applied modelling. For (non-research) estuary modelling scales are typically of the order of 50-100m in estuaries (and greater for large systems)

The inability of applied models to reproduce the small-scale variation in bed levels can result in a poor overall description of flow through grid cells representing flow through highly varied since the bed is represented by a single level throughout the cell. A single level cannot both adequately represent the total storage and the deepest channel through the cell. Usually the bed level is "averaged" meaning that the model represents flow through the grid cell later in the tide than the real situation. This can result in a poor representation of flow through the (saltmarsh or mudflat) system as a whole especially as it drys and wets. Moreover in an estuary system or tidal inlet dominated by significant and small-scale bathymetric variation these problems can result in a generally poor reproduction of flows in the system.

The normal course of action open to the numerical modeller is to enhance the grid resolution over the (dendritic) mudflat/saltmarsh up to the point where the flow within the system becomes acceptably similar to the observations. However higher grid resolutions lead to larger numbers of nodes and smaller elements, which can lead to unacceptably long run times.

The algorithm described below includes the effect of the small-scale bathymetric variation on flows without increasing the mesh resolution. This type of approach is termed "sub-grid" modelling.

Improvement in understanding
The new method improves on existing methods because:

- it can significantly improve the accuracy of the flow model, especially within the saltmarsh;
- the increase in run times is of the order of 15%-25%.

Implementation
The algorithm makes use of the TELEMAC-2D flow model software which allows the specification of the porosity of flow within a model element. However, algorithm is written in a step-by-step "recipe" style, which can easily be coded for any computer application (assuming porosity is included in the form of the continuity and momentum equations which the model is solving).

The TELEMAC-2D software implements a FORTRAN file (called "princi.f") which governs the way initial and boundary conditions, etc, are implemented within the model. This princi.f file also implements the routine that specifies porosity if required. The algorithm is implemented within two of the subroutines which form the princi.f

file: CORFON (where the initial bathymetry is specified) and POROS (where the porosity is set).

Algorithm

Inputs
High resolution bathymetry data set (m datum)

Outputs
Minimum bed level for each model node (m datum)
Porosity for each model element (no units)

1 Using the appropriate mesh generator, generate the mesh and bathymetry for the available data set
2 Calculate the required search radius. This should be done by trial and error but as a starting point the following search radius is suggested (for meshes with triangular elements)

$$\mathrm{SR} = \frac{1}{2\sqrt{3}} < \text{grid resolution} >$$

3 Locate all the bathymetric points within a certain search radius for each model node
4 Redefine the bathymetry so that, as long as one data point or more is found within the search radius, the bathymetry at each model node is altered to the lowest elevation from those points within the search radius.
5 Define two arrays:
ncount(i) , the number of bathymetric points corresponding to node i
zcount(i,k) , the level of the k^{th} bathymetric point at node i
6 Sort the values of zcount(i,k) so that the lowest elevation is zcount(i,1) and the highest elevation is zcount(i,N)
7 On each time step …

For each node …

Calculate

$$A(i) = \sum_{k=1,j} k.\min(zcount_{k,i}, fs_i) \qquad P(i) = \max\left(\frac{A(i)}{H(i)}, 0.5\right)$$

where j is given by $zcount_{i,j-1} < fs_i < zcount_{i,j}$;
$zcount_{k,i}$ is the k^{th} elevation for the i^{th} node ;
fs_i is the free surface elevation at node i;
P is the porosity associated with node i.

(necessary for TELEMAC software)
Calculate the porosity of each element

$$PE_m = \tfrac{1}{3} P_{m,1} + \tfrac{1}{3} P_{m,2} + \tfrac{1}{3} P_{m,3}$$

where PE_m is the porosity associated with the m^{th} element;
$P_{m,1}$ etc are the porosities associated with the three nodes corresponding to the m^{th} element.

Limits of applicability
The algorithm is applicable where there is high resolution bathymetric data (ie where the resolution of bathymetric measurements is significantly greater than the model grid resolution).

Validation
The effectiveness of the algorithm was investigated using a TELEMAC-2D model of Salcott Creek in the Blackwater Estuary (Spearman et al, 2004, this report). Model results derived using the algorithm were compared objectively (using the Brier Skill Score method) against model results derived those derived without the method and with a reference data set generated using a very high resolution model.

References
Hervouet J, Samie R and Moreau B (2000), Modelling urban areas in dam-break flood-wave numerical simulations, International seminar and workshop on rescue actions based on dam-break flood analysis, 1-6 October 2000, Seinäjoki, Finland.

HR Wallingford (2001), Sustainable Flood Defences. Monitoring of Retreat and Recharge Sites, Project Number MRD 21110, Abbott's Hall, Numerical Modelling, HR Wallingford EX Report 4367, August 2001.

Spearman J R, Baugh J and McCoy M J (2004), Use of sub-grid approaches in the modelling of estuaries with salt marsh systems, HR Wallingford Report TR138, January 2004.

Sutherland, J. and Soulsby, R.L., (2003). Use of model performance statistics in modelling coastal morphodynamics, Proceedings of the International Conference on Coastal Sediments 2003, CD-ROM Published by World Scientific Publishing Corp. and East Meets West Productions, Corpus Christi, Texas, USA. ISBN 981-238-422-7.